Universität Bremen
Faculty of Environmental Physics

Master Thesis

Medical ^{131}I in Weser water

Maria-Evangelia Souti

1st supervisor: Dr. H. Fischer
2nd supervisor: PD Dr. G. Kirchner

Bremen, August 10th 2012

Contents

Acknowledgements

This study would not have been possible without the contribution of several people to whom I express my gratitude.

First I would like to thank Dr. Helmut Fischer, for giving me the opportunity to work in the Radioactivity Group. The project he offered me, apart from being interesting, it was a full experience of collecting data, analyzing them, testing methods, experimenting in the lab and finding solutions for problems that came up. All this work could have been impossible without his guidance and coordination.

My appreciation for all the members of the group, every single one of them was all this time by my side helping me in any way they could. The group chemists, Edda Toma and Regine Braatz assisted me in the chemistry lab in every way possible, introduced me to chemical methods and solutions and made me love chemistry once more! The students Felix Rogge and Dominik Höweling were always willing to help me sampling. Homa Ghasemifard was the best company I could have in my office; supporting me and trying to cheer me up.

My gratitudes to the Lab Technician Bernd Hettwig for helping me not only around the radioactivity lab, but also in the sampling procedure.

Special thanks to Dr. Volker Hormann and to my tutor Susanne Ulbrich for devoting their time to understand and assist me in my work.

Last but not least, I'm thankful to my family, my boyfriend and my friends for always inspiring, supporting and encouraging me.

Abstract

Nuclear medicine plays an important role within man made radioactive environmental impacts. ^{131}I is the most used radioisotope in nuclear medicine. At the same time is one of the most important short-lived nuclear fission products with its own environmental impact (e.g. Chernobyl, Fukushima).

Former studies on the environmental pathway of ^{131}I into the Weser River have identified the activity concentration of the radionuclide in river sediments and indicated the Waste Water Treatment Plant (WWTP) as the primary source.

This study focuses in the detection, determination and transport of the radionuclide in the river water since it represents the connecting link between the WWTP and river sediments.

Prerequisite for this investigation is the application of a chemical extract procedure, making possible the detection of low concentrations of ^{131}I in the river water.

The results of this study will be used further on, in the assessment of a radionuclide transport model developed for the Weser River.

List of figures

List of tables

Introduction

^{131}I as a major uranium, plutonium fission product was a significant contributor to the health hazards from open air atomic bomb testing in the 1950s and from the Chernobyl disaster and Fukushima disasters (**U.S. Environmental Protection Agency, 2012**). Apart from this role, ^{131}I is also known as an important radiopharmaceutical.

Along with its useful beta emission, ^{131}I has short radioactive (8 days) and biological half lives (100 days), allowing it to be extensively in nuclear medicine. Its tendency to collect in the thyroid gland makes it especially useful for treatment of thyroid problems.

^{131}I was first introduced in 1946 for the treatment of thyroid cancer, and remains the most efficacious method for the treatment of hyperthyroidism and thyroid cancer (**U.S. Environmental Protection Agency, 2012**). In the case of cancer, the radioactive iodine is prescribed after the surgical removal of the thyroid in order to completely destroy any remaining thyroid tissue (**Jardin C., et al., 2009**).

^{131}I has become the most abundant radiopharmaceutical representing close to 90% of all radiotherapies (**Barquero R. et al, 2008**). In Germany only at 2009, 40154 iodine treatments we performed **(www.g-drg.de, 2012).**

Motivation

Several papers deal with environmental pathways of ^{131}I **(Fischer H. et al. 2009, Barquero R. et al. 2008, Nakamura A. et al. 2005, Sundell S.et al. 2008)**

Already from 2000, in the Radioactivity Measurements Laboratory, in a regular basis (approximately 4 times a year) effluent from Bremen WWTP was measured for the surveillance network for environmental radioactivity (IMIS), and its ^{131}I activity concentration was determined (appendix 4).

The beginning of the investigation of ^{131}I in the river was done with Susanne's Ulbrich master thesis at 2008. In her master thesis she managed to find ^{131}I in sediment samples to the WWTP wider area and connect this activity to the WWTP effluent. The work continued a year later with Philip Lysogne. He collected 25 sediment samples along the Weser River, starting from Bremen Centre till Bremerhaven, in which ^{131}I was found. The activity concentration of ^{131}I had its highest value in the area next to the WWTP and decreased by increasing distance from it. ^{131}I in sediments was also found along the river up to 10 km distance from the WWTP to the direction of the city and 20 km to the direction of the coast. More information can be found in appendix 1.

The goal of this study is to investigate the radioiodine concentration in the Weser river water, the link between WWTP outflow (source) and sediments (sink). At the same time a simple model for the radionuclide transport in the river water and sediments will be created. The activity concentration of ^{131}I detected in the water, along with the already known in sediments will be used further in the assessment of the model.

Chapter 1

Theoretical Background

1.1 Radioactive decay

Radioactive decay is the process in which a spontaneous change occurs inside the nucleus and results in the emission of particles or electromagnetic radiation. The radioactive decay is driven by mass change of the nucleus, called parent isotope, resulting in lowest energy in the products. This energy difference is determined by Einstein's equation:

$$\Delta E = \Delta m \cdot c^2$$

The activity of a radioactive source is defined from the number of disintegrations per second and measured in Becquerel: 1Bq= 1disintegration/s. An older unit is Curie:
1 Ci= 3.7×10^{10} Bq.

There exist 3 main decay modes: alpha, beta and gamma decay.

Alpha decay: The emission of alpha particles is a common phenomenon in heavy nuclei (proton number Z> 83), where an alpha particle is emitted (^{4}He nucleus) by penetrating the Coulomb barrier of the heavy nucleus through quantum mechanical tunneling.

$$^{A}_{Z}X \rightarrow ^{A-4}_{z-2}Y + \alpha\left(^{4}_{2}He\right) + E$$

The alpha particles are monoenergetic with kinetic energy ranging between 2-10MeV, depending on the parent isotope. A graphic example follows with the emission of an alpha particle from ^{240}Pu nucleus resulting to ^{236}U nucleus.

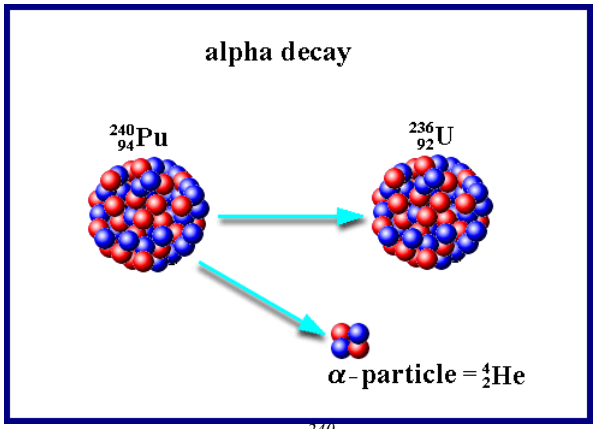

Figure 1: Alpha decay of ^{240}Pu ***(Homepage wissenschaftlicher Themen, 2002)***

In many cases the emission of an alpha particle can result in excited states of the daughter isotope.

Beta decay: The radioactive decay process resulting in the emission of beta particles is called beta decay and can be subdivided in 2 categories β^- and β^+ decays.

β⁻ -decay: The emission of β⁻-particles is caused by the transformation of a nucleus ${}^{A}_{Z}X$ with Z protons and (A-Z) neutrons, to nucleus ${}^{A}_{Z+1}Y$ with an extra proton (Z+1), a neutron less (A-Z-1) and the same mass number (A) accompanied the emission of an electron and an antineutrino:

$$ {}^{A}_{Z}X \rightarrow {}^{A}_{Z+1}Y + e^{-} + \overline{\nu}_{e} + E $$

reaction equivalent with the transformation of a neutron to a proton inside the nuclear field:

$$ n \rightarrow p + e^{-} + \overline{\nu}_{e} $$

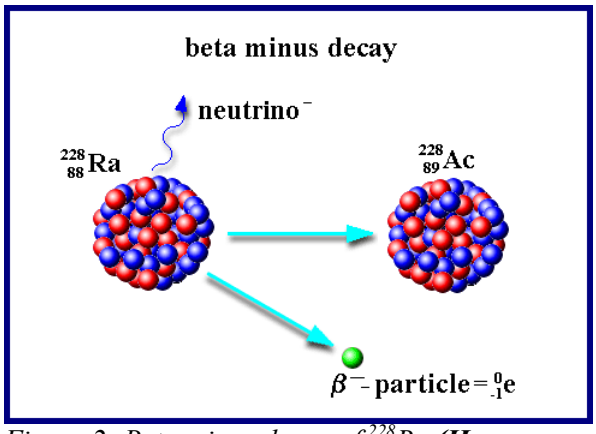

Figure 2: Beta minus decay of ^{228}Ra ***(Homepage wissenschaftlicher Themen, 2002)***

β⁺ -decay: The emission of β⁺ -particles is caused by the transformation of a nucleus ${}^{A}_{Z}X$ with Z protons and (A-Z) neutrons, to nucleus ${}^{A}_{Z-1}Y$ with an proton less (Z-1), an excess neutron and the same mass number (A) accompanied the emission of an positron and a neutrino:

$$ {}^{A}_{Z}X \rightarrow {}^{A}_{Z-1}Y + e^{+} + \nu_{e} + E $$

reaction equivalent to the transformation of a proton to a neutron:

$$ p \rightarrow n + e^{+} + \nu_{e} $$

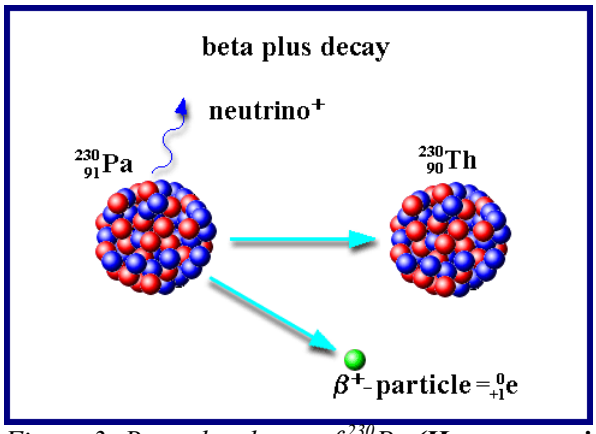

Figure 3: Beta plus decay of ^{230}Pa ***(Homepage wissenschaftlicher Themen, 2002)***

The energy range of the emitted electrons/positrons is continuous, from some keV to the maximum energy (E_{max}), some MeV, which corresponds to the energy difference between parent and daughter isotopes. The continuous energy spectrum of the beta

particles is caused by the distribution of energy between the produced particles (electron-antineutrino, positron-neutrino).

Electron capture: As a competing process to β+ decay, in neutron deficient nuclide, the electron needed to convert the proton is captured by the nucleus from one of the extra nuclear electron shells.

$$ {}^{A}_{Z}X + e^{-} \rightarrow {}^{A}_{Z-1}Y + \nu_e + E $$

$$ p + e^{-} \rightarrow n + \nu_e $$

Gamma decay: The emission of gamma radiation (photons) is caused during the transition of an excited nuclear state ${}^{A}_{Z}X^{*}$ to another energy state (intermediate or ground state) of the same nucleus ${}^{A}_{Z}X$:

$$ {}^{A}_{Z}X^{*} \rightarrow {}^{A}_{Z}X + \gamma $$

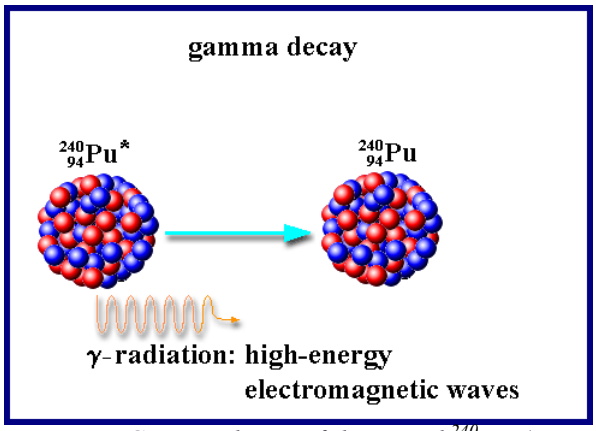

Figure 4: Gamma decay of the exited ^{240}Pu ***(Homepage wissenschaftlicher Themen, 2002)***

The energy of the emitted gammas is monoenergetic, characteristic for the parent nuclide and their energy range is between some keV and several MeV.

The de-excitation of a nucleus can also occur through internal pair production (quite uncommon procedure) and internal conversion (the excitation energy is transferred to an atomic electron which is ejected from the atom).

X rays: X-rays are electromagnetic radiation emitted in transitions of the atomic electrons between different states in an atom. They are monoenergetic and their energy is equal to the difference between electron energy levels. They appear in gamma spectra as a result of rearrangement of extranuclear atomic electrons after electron capture and internal conversion.

Several other decay modes exist, such as the emission of a proton or neutron, or the spontaneous fission in which the parent nucleus spontaneous breaks down into smaller nuclei and few isolated nuclear particles. In the following figure a chart of the nuclides for decay modes is presented.

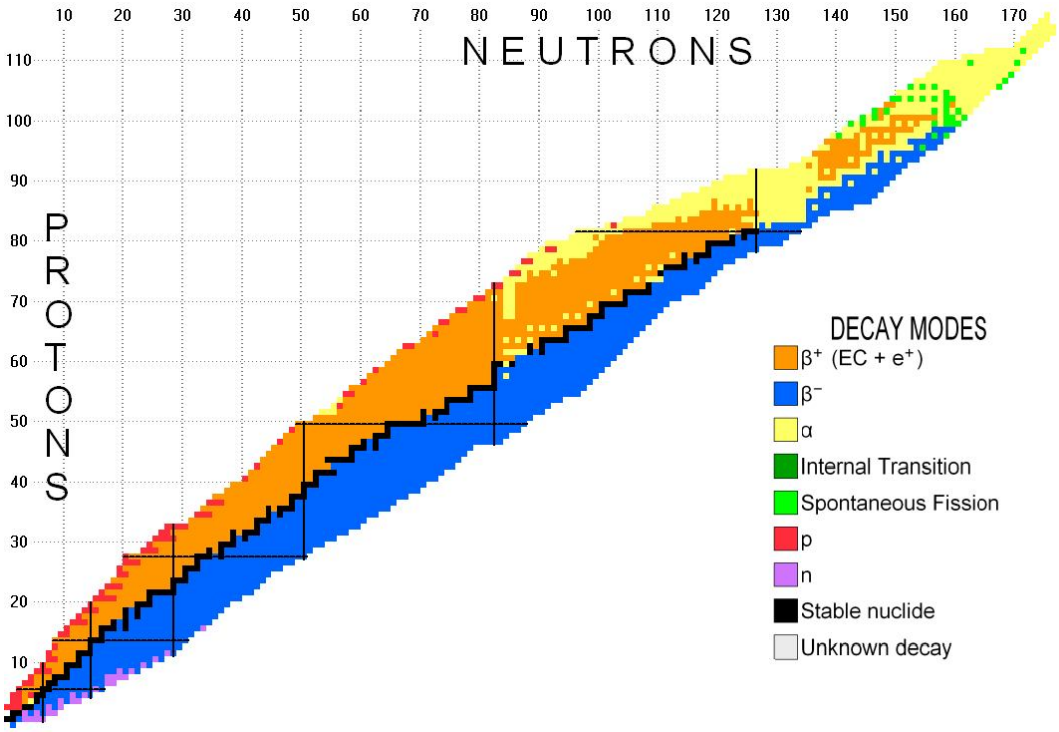

Figure 5: Nuclide chart for different decay modes ***(Audi G. et al., 1997).***

1.2 Radioactive iodine

Radioactive ^{131}I was discovered by Glenn T. Seaborg and John Livingood at the University of California-Berkley in the late 1930`s. Most of its production is in Research Reactors by irradiating TeO_2 targets with neutrons. ^{130}Te captures the neutron and transforms to ^{131}Te which decays to ^{131}I with a 25 min half life:

$^{130}Te\ (n, \gamma) \rightarrow {}^{131}Te \rightarrow {}^{131}I$

After approximately 2 days of cooling, TeO_2 is heated at about 730^{o}C and ^{131}I is released, 99% of which, through chemical distillation, is absorbed as sodium iodide.

Figure 6: Sodium Iodide Capsules ***(Covidien Pharmaceuticals,2012)***

^{131}I is also produced by fission of uranium atoms during operation of nuclear reactors and by plutonium (or uranium) in the detonation of nuclear weapons.

^{131}I environmental pathway

Usually sodium iodide capsules of several GBq are given to patients for the treatment of hyperthyroidism and thyroid cancer.

After a patient undergoes an iodine treatment, the activity which is not retained from the thyroid is excreted through the urinary system to the sewage as a radioactive effluent.

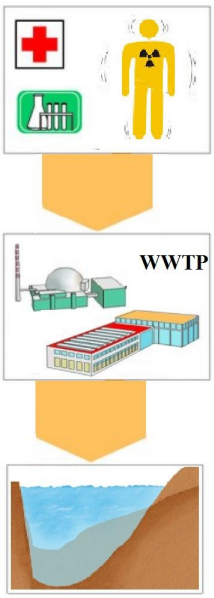

In Germany, the maximum ^{131}I body activity of a patient released from the hospital is 250 MBq. The amount of this activity is comparable to the reported total release of ^{131}I from all commercial nuclear power plants to ambient air and water in 2006. **(Fischer H. et al., 2009)**

The sewage material arrives to the Bremen WWTP with a mean activity of 450±11 mBq/l **(S. Ulbrich master thesis, 2008)**
and exits approximately half of it (234±4 mBq/l) (IMIS data- appendix 4) as effluent in the river with a mean flow rate of 1.3m^3/s (WWTP data, appendix 5)

However since the flow rate of the river is approximately 200 times more **(Rijn L., 2011)** after dilution with the river water, the concentration is below the detection limit of the employed gamma spectrometers.

Figure 7: ^{131}I environmental pathway

^{131}I decay process

^{131}I with a half life of 8.02 days, with a β^- decay process, decays into an exited state of ^{130}Xe, which in turn 81.7% of the times goes to a ground state of ^{130}Xe by emitting a gamma line of 364.5keV:

$$^{131}\mathrm{I} \rightarrow \beta^- + \overline{\nu}_e + {}^{131}\mathrm{Xe}^* + \mathrm{K.E.\ (606\ keV)}$$
$$^{131}\mathrm{Xe}^* \rightarrow {}^{131}\mathrm{Xe} + \gamma\ (364\ \mathrm{keV}).$$

and 7.17% of the times goes to a ground state of ^{130}Xe by emitting a gamma line of 636.9 keV:

$$^{131}\mathrm{I} \rightarrow \beta^- + \overline{\nu}_e + {}^{131}\mathrm{Xe}^* + \mathrm{K.E.\ (333\ keV)}$$
$$^{131}\mathrm{Xe}^* \rightarrow {}^{131}\mathrm{Xe} + \gamma\ (636\ \mathrm{keV}).$$

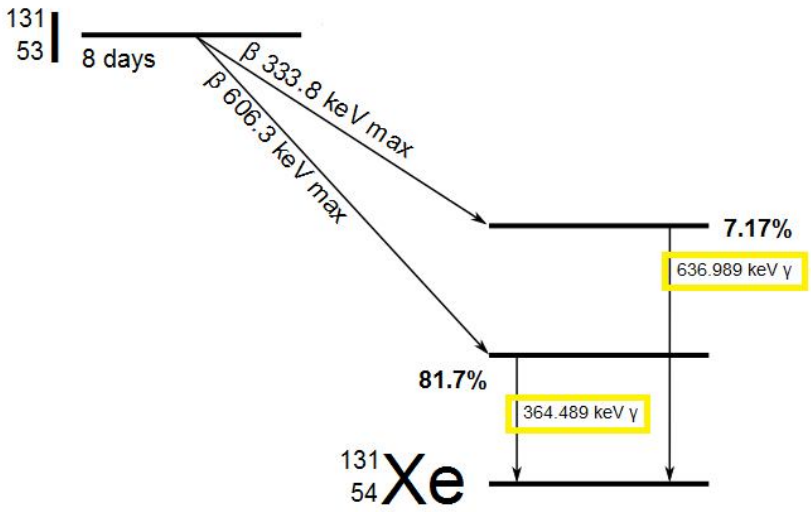

Figure 8: Simplified ^{131}I decay scheme.

Although those two are the most prominent gamma lines of the ^{131}I decay, they are not the only ones. The following tables 1, 2 present all the gamma and X-rays lines of ^{131}I with their corresponding abundance:

Tables 1 and 2: Gamma and X-ray lines from ^{131}I decay. **(Isotope Library, 2004)**

Gammas from ^{131}I (8.02070 d)

Eγ (keV)	Iγ (%)	Decay mode
80.185	2.62	β^-
85.9	0.00009	β^-
163.930		β^-
177.214	0.270	β^-
232.18	0.0032	β^-
272.498	0.0578	β^-
284.305	6.14	β^-
295.8	0.0018	β^-
302.4	0.0047	β^-
318.088	0.0776	β^-
324.651	0.0212	β^-
325.789	0.274	β^-
358.4	0.016	β^-
364.489	81.7	β^-
404.814	0.0547	β^-
503.004	0.360	β^-
636.989	7.17	β^-
642.719	0.217	β^-
722.911	1.773	β^-

X-rays from ^{131}I (8.02070 d)

E (keV)	I (%)	Assignment
3.633	0.0086	Xe L_l
3.955	0.0040	Xe L_η
4.093	0.024	Xe $L_{\alpha 2}$
4.105	0.215	Xe $L_{\alpha 1}$
4.414	0.133	Xe $L_{\beta 1}$
4.451	0.0127	Xe $L_{\beta 4}$
4.512	0.021	Xe $L_{\beta 3}$
4.569	0.00170	Xe $L_{\beta 6}$
4.714	0.042	Xe $L_{\beta 2}$
5.034	0.0186	Xe $L_{\gamma 1}$
5.307	0.0033	Xe $L_{\gamma 2}$
5.307	0.0049	Xe $L_{\gamma 3}$
29.112	1.43E-04	Xe $K_{\alpha 3}$
29.461	1.40	Xe $K_{\alpha 2}$
29.782	2.59	Xe $K_{\alpha 1}$
33.562	0.238	Xe $K_{\beta 3}$
33.624	0.459	Xe $K_{\beta 1}$
33.881	0.00467	Xe $K_{\beta 5}$
34.419	0.139	Xe $K_{\beta 2}$
34.496	0.0269	Xe $K_{\beta 4}$

As mentioned before, the beta decay gives a continuum spectrum with a range of zero to maximum energy, making it difficult to identify ^{131}I in samples. Since ^{131}I is also a gamma emitter, we use its gamma ray to identify it and determine its activity in the sample. For this reason we use gamma spectroscopy.

1.3 Gamma spectroscopy

Gamma spectroscopy is based in the indirect ionization the photons cause when they interact with matter. There are 3 main mechanisms of interaction:

Photoelectric absorption:
In the photoelectric absorption process, a photon undergoes an interaction with an absorber atom in which the photon completely disappears by transferring all its energy to an atomic electron which is ejected from its shell.

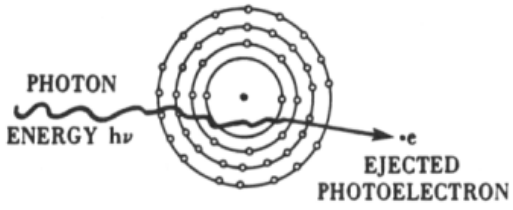

Figure 9: Photoelectric absorption
(www.fesaus.org, 2010)

Compton scattering:
The interaction process of Compton scattering takes place between the incident photon and an electron in the absorbing material. The photon transfers part of its energy to the electron which is ejected from its shell and the remainder appears as a secondary photon.

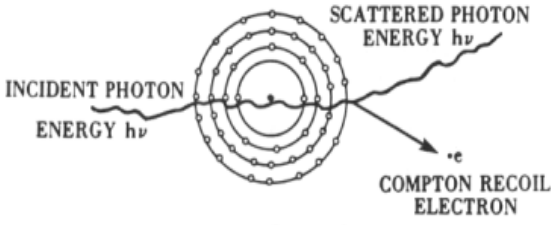

Figure 10: Compton scattering
(www.fesaus.org, 2010)

Pair production:
If the gamma ray energy exceeds twice the rest electron mass (1.02MeV), the process of pair production is energetically possible. In the interaction (which must take place in the Coulomb field of the nucleus), the photon is converted into a positron-electron pair.

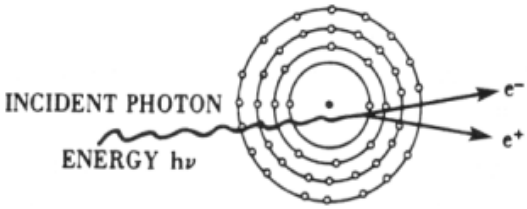

Figure 11: Pair production
(www.fesaus.org, 2010)

Experimental setup

A gamma spectroscopic system consists of a semiconductor detector, electronics to collect and process the signal and a computer with special software which analyses, displays and stores the spectra.

Semiconductor detector: When a photon deposits energy in a semiconductor detector, equal number of conduction electrons and holes are formed within a few picoseconds. More precisely the interaction of a gamma ray with the semiconductor material will produce primary electrons with energies larger than thermal energies, making them capable to rise from the valence band to the conduction band leaving holes in the valence band, as shown in the figure below:

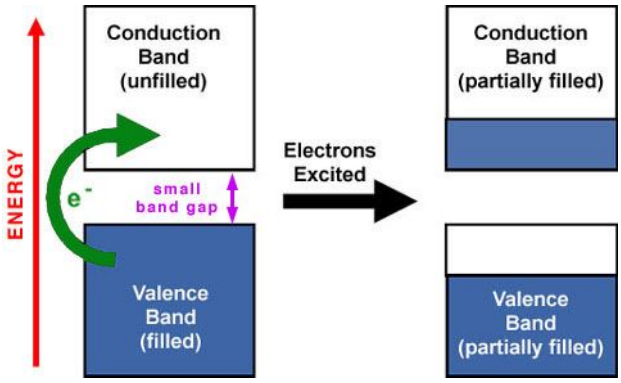

Figure 12: In a semiconductor, the band gap is small enough that electrons can be moved from the valence band to the conduction band. ***(Department of Chemistry, Washington University in St. Louis, 2002)***

When high voltage is applied to the crystal, the electrons in the conduction band can respond to electric field in the detector and therefore move to the positive contact that is creating the electric field. The hole in the valence band is filled in with an adjacent electron. This shuffling creates a positive charge to the negative contact. Both electron in negative contact and hole in positive contact create the electrical signal which is sent to the electronic system for processing and analysis. A typical semiconductor detector is illustrated below:

Because of the small bandgap (0.7eV), room temperature operation is impossible since thermally induced current would result from electrons capable of jumping the small energy gap. Instead germanium detectors need to be cooled to reduce the leakage current. The temperature is reduced to 77 K through the use of a dewar in which reservoir of liquid nitrogen is kept in contact with the detector.

Figure 13: Typical germanium detector with lead shielding attached to liquid nitrogen reservoir (bottom).

Electronics: The objective of the electronic system is to transfer the electrical charge which is proportional to the amount of photon energy absorbed by the detector, from the detector to the Multi Channel Analyzer (MCA) with as little alternation as possible.

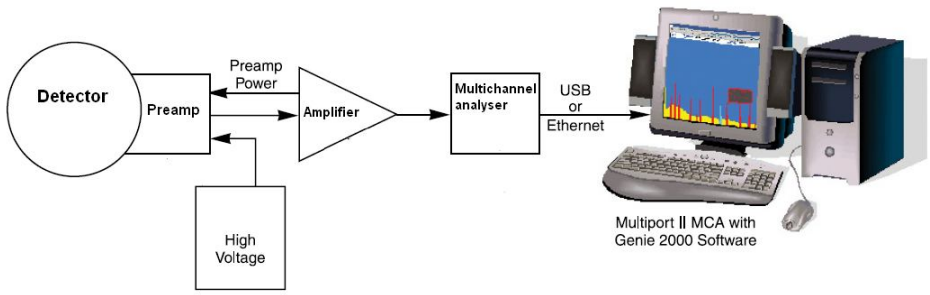

Figure 14: Simplified electronic system **(Canberra Industries, 2010).**

The collected charge is converted into a voltage pulse whose shape is changed and size increased in the amplifier with amplitude proportional to the original photon energy. The voltage pulse is then converted to digital information in the analog to digital converter (ADC) and transferred to MCA. The MCA, in simplest form, analyses a stream of voltage pulses and sorts them by pulse height and counts the number of pulses within individual pulse intervals and stores them as a "spectrum" of number of events versus pulse-height which can be related to energy. The stored spectrum may then be displayed and analyzed through a computer system with special equipped software.

Spectrum: A spectrum corresponding to one of the samples we collected is presented here:

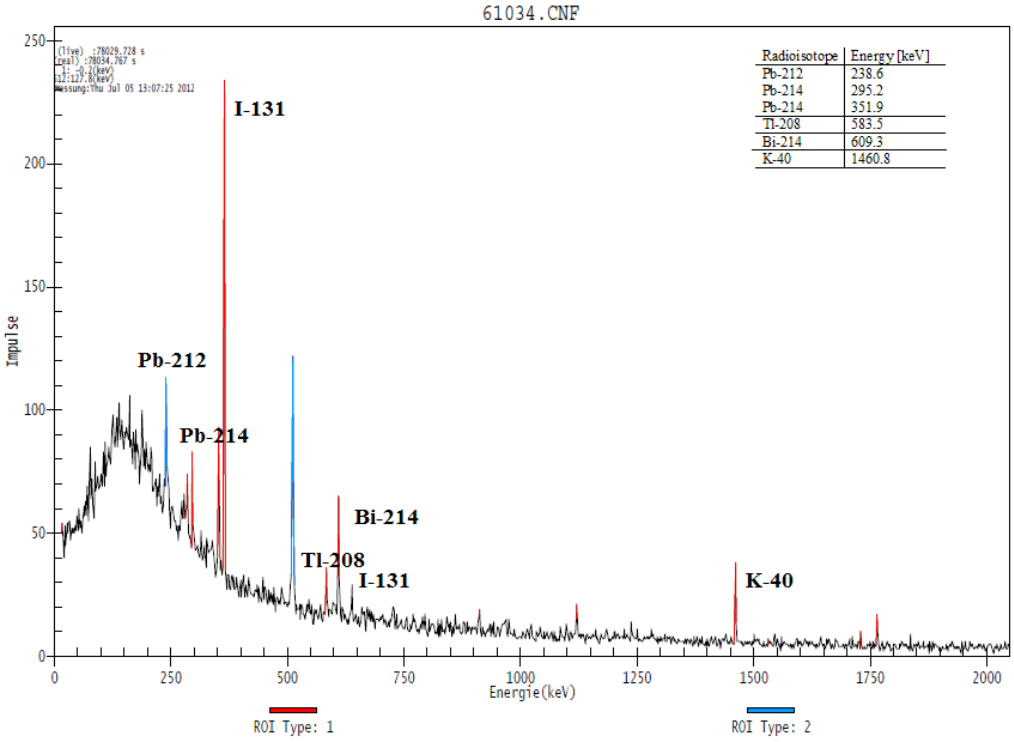

Figure 15: Typical river water spectrum for sampling location close to the WWTP

The physics behind the form of this spectrum is closely related to the mechanisms of photons interacting with matter as explained in previous paragraph.

Ideally the photon performs photoelectric absorption and the emitted electron transfers all its energy to the electric pulse and as a result the current which results us very representative of the incident photon's energy and very specific for the nucleus from which is was emitted. This characteristic allows us to identify different isotopes in spectra. In this spectrum apart from the ^{131}I peaks at 364.5 keV and 637.0 keV, we see other isotopes such as ^{212}Pb with a peak at 238.6 keV, ^{214}Pb with peaks at 295.2 and 351.9 keV, ^{208}Tl with peak at 583.5 keV, ^{214}Bi with peak at 609.3 keV and ^{40}K with its characteristic peak at 1460.8 keV. All these "additional" isotopes have natural origin and the might originate from our water sample, or from the material used for the chemical extraction and preparation of the sample or from the environment of the measurement. In order to eliminate a possible false interpretation of our ^{131}I activity concentrations we performed along measurements, with of course the background measurement (an example of which is presented in next paragraph), of material used for the chemical extraction and preparation of the sample. The spectra are given in the appendix 7 and as expected they contain natural origin isotopes and undetectable ^{131}I.

Most of the times, photons undergo Compton scattering and the resulting pulse is unspecific. The lowest part of our spectrum, which provides no information for the isotopes, is caused by Compton scattering.

In the case of a pair production, both electron and positron will slow down inside the material and annihilate, giving the so called annihilation peak at 511 keV, common feature in gamma spectra.

Spectrum analysis- Background subtraction: When analyzing a spectrum our first task is to subtract the background spectrum, an example of which is given below:

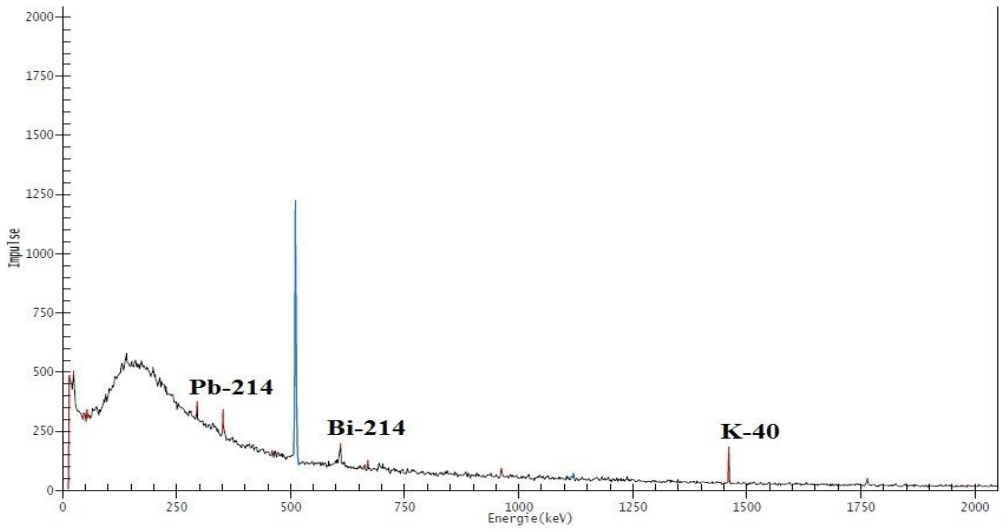

Figure 16: Typical background spectrum

We observe again apart from the annihilation peak, several other peaks belonging to natural occurring isotopes such as ^{40}K, ^{214}Pb and ^{214}Bi.

Since the radioactive decay follows a Poison distribution, which is the limiting case of a binomial distribution for an infinite number of time intervals, for any counting experiment the result of which is governed by Poisson distribution the standard deviation is $\sigma = \sqrt{N}$. This states that in a case of repetition of the experiment about 2/3 of the time would result in the N±σ range. If we assume equal counting times, then the net counts are given as

$$N = N_{tot} - N_{bg} \qquad \text{(i)}$$

and the standard deviation is then given as:

$$\sigma = \sqrt{\sigma_{tot}^2 + \sigma_{bg}^2} = \sqrt{N_{tot} + N_{bg}} \qquad \text{(ii)}$$

In the case where the background has a slope, we need to determine the counts in both sides of the peak and average.

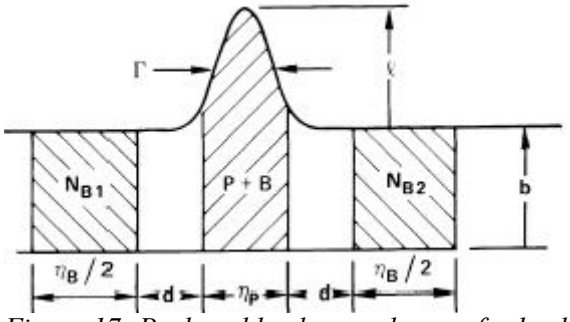

Figure 17: Peak and background areas for background subtraction ***(Fischer H., 2003)***

Spectrum analysis-Calibration:

- Energy calibration allows the gamma ray spectrum to be interpreted in terms of energy, through a linear relationship by relating the peak position in the spectrum and the corresponding gamma ray:

$$E = A\,(ch) + B \qquad \text{(iii)}$$

where ch=channel number, E the gamma ray energy, A the gradient of the linear relationship and B its offset.
Thus the energy vs. channel number can be directly read out.

- Efficiency calibration derives a relationship between the number of counts and the emitted photons. As shown in the next figure, geometry of the sample plays an important role to the energy depended efficiency.

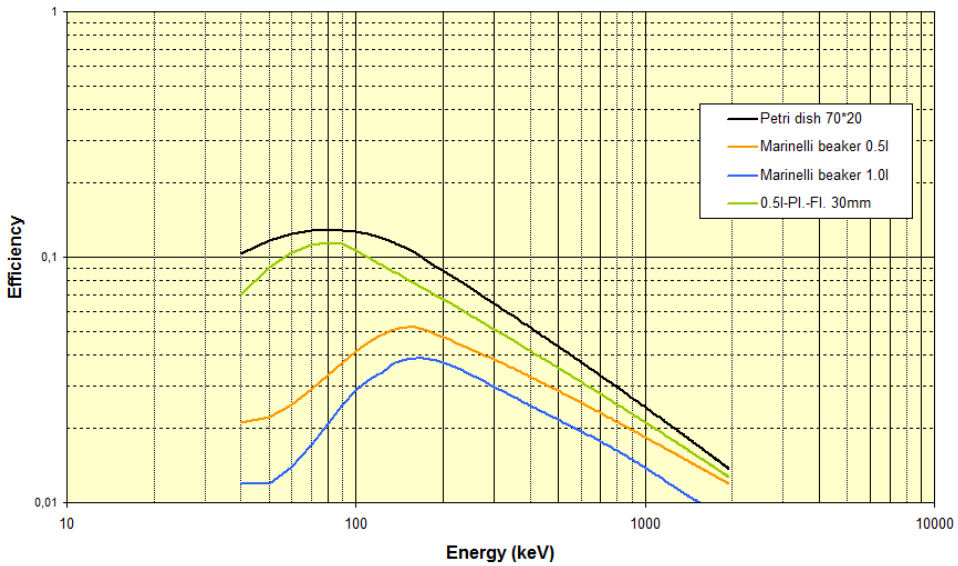

Figure 18: Efficiency calibration curves for different geometries ***(Radioactivity measurements laboratory- Data generated by Genie 2000 software).***

Also the density of the samples and the distance from the detector strongly affect the efficiency. In a more quantitative way:

$$\varepsilon(E) = \frac{N}{t \cdot f \cdot A} \rightarrow A = \frac{N}{\varepsilon \cdot f \cdot t} \rightarrow A = \frac{R}{\varepsilon \cdot f} \qquad \text{(iv)}$$

where A the activity,
f the emission probability of the observed gamma emission,
N the counts in peak
ε(E) the energy depended peak efficiency and
R=N/t the peak count rate.

Spectrum analysis-Detection limit:

As detection limit we define the smallest concentration of radioactivity in a sample that can be detected with a 5% probability of detecting radioactivity by error when none was present (Type I error) and a 5% probability of not detecting radioactivity when it is in fact present (Type II error). The detection limit can be improved by increasing the efficiency, the measurement time or the sample size.

This is the reason we apply a chemical extraction method, in order to reduce the volume of the sample containing the ^{131}I. The following table indicates the detection limit different measurement geometries can reach for a sample of 20 liters original volume and a measuring time close to 24 hrs.

Table 3: Detection limits for different geometries

Geometry	Detection limit (mBq/l) 20lt-24hrs
2 Lt Marinelli	5.0
1 Lt Marinelli	3.5
0.5 Lt Marinelli	2.7
0.5 Lt Plastic Bottle (30mm filling height)	2
Petri dish (70x20mm)	1.6
Filter (d=38mm)	0.6

The ideal geometry is to use a 38mm filter which gives us lower than 1 mBq/l activity concentration, while 1 liter Marinelli beaker gives us almost 6 times higher detection limit.

Chapter 2

Chemical extraction methods for determination of ^{131}I in Weser water

In order to detect low concentrations of ^{131}I in Weser River water, we need to apply a chemical extraction method which provides the lowest detection limit as possible.

A literature survey indicated several possible methods to chemical extract the ^{131}I from water leading to a reduction of the original volume of the sample and thus in a decrease of the detection limit. As discovered both EPA method #902.0 **(EPA 1980)** and "Parekh's, Bari's and Harris's chemical extraction method" **(Parekh P. et al, 2002)** are inadequate methods to achieve this limit (1 $pCi \cdot l^{-1}$ or 0.037 $Bq \cdot L^{-1}$ and 0.5 $pCi \cdot l^{-1}$ or 0.0185 $Bq \cdot L^{-1}$ for 200 min counting time respectively). Especially the EPA method requires at the same time 2 days of chemistry, which makes it tedious and time consuming.

On the other hand, 2 different methods proposed by **Mundschenk 1993**: "Verfahren zur Bestimmung von Iod-131 in Oberflächenwasser" (Method for determination of ^{131}I in surface water) and "Verfahren zur gammaspektrometrischen Bestimmung von Radionukliden in Oberflächenwasser" (Gamma spectrometric method for determination of radionuclides in surface water), appeared more simple and with the ability to reach lower detection limits, 0.6mBq/l and 3.5mBq/l respectively for a 20 l water sample and approximately 24 hours measuring time. Both these methods we tested in the framework of this study, however, for reasons explained further on, only the second method was used to determine the concentration activity in the Weser river water.

2.1 Method for determination of ^{131}I in surface water

The method as proposed by **Mundschenk 1993** (Verfahren zur Bestimmung von Iod-131 in Oberflächenwasser) is based in the extraction of the iodine by a silver chloride filter. A step by step complete description of the method follows. For smaller or larger sample volumes, thus reduced or increased sensitivity, the additions of chemicals have to be adjusted properly.

1. Radiochemical separation- Separation/Deposition of ^{131}I on silver chloride filter

For a 20 liter river water sample the procedure is as follows:

1. In a plastic container (volume 25 litres), we add 6 litres of the sample and the following chemicals:
   - 2 ml of potassium iodide solution (20mg I^-)
   - 0.4 g sodium sulfite

- 20 ml aluminium sulfate (0.3 g Al^{3+})

2. We add the remaining sample of 14 litres and acidify it with concentrated sulfuric acid (18 mol l^{-1}) until it reaches a ph value of 1 to 2 and stir to homogenize well.

3. Afterwards we add 40 to 80ml of saturated sodium carbonate solution until we reach ph value 8 to 9.

4. We stop the stirring and let the sample precipitate for 2 hours, although it can serve better overnight.

5. After the precipitation occurs, the supernatant is decanted or siphoned off and transferred in a second plastic container (volume 25 Litres). The precipitate, which can contain ^{131}I in organically bound form or bound to particulate matter, is measured in wet or dry form with a semiconductor detector. Then the decanted sample is acidified with some concentrated nitric acid (10 mol l^{-1}) to a ph value of 1.

6. Preparation of the Silver Chloride filter
- 24 ml of silver nitrate solution (240 mg Ag^{+}) are mixed with weak nitric acid solution until the pH value is 1 to 2. Then about 32 ml of saline solution (105 mg Cl^{-}) are added and the mixture is left to precipitate in room temperature.

- The precipitate is immediately sucked through a filter (eg. Schleicher & Schüll, Nr. 8) and washed with some nitric acid. In our case a filter (diameter of the filter surface: 38 mm) is used.

7. The clear, acidified sample is sucked afterwards at full suction power of a vacuum pump through the freshly prepared filter. In order to avoid losses of weight by washing out, the filter is always kept covered with a 2 to 3 cm high layer of liquid. Depending on the composition of the samples, 20 Litres in 1 to 2 hours are interspersed. In highly polluted water samples with suspended solids, the filter plate must be renewed if necessary, so that the flow speed does not drop too much and the time required for the separation of ^{131}I does not rise too much. In the following figure the filtering setup is illustrated, for a 38mm filter.

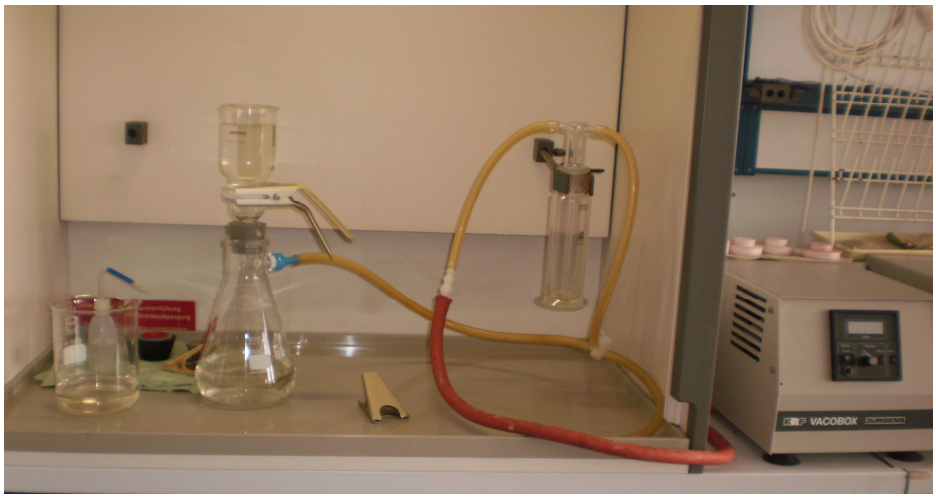

Figure 19: Filtering equipment for a 38mm diameter filter. On the right the vacuum pump is shown.

8. After the sucking of the sample, the silver chloride filter is washed off in a porcelain dish with ammonium hydroxide solution (10 mol l^{-1}) and transferred into a beaker. From the turbid solution by addition of nitric acid (4 mol l^{-1}), silver iodide is precipitated again. The precipitation is over a Hahn'sche filter (diameter: 40 mm, filter surface area: 12.6 cm^2). The filter is then washed with some nitric acid (1 mol l^{-1}) and then with a mixture ethanol/water (1:1(v/v)). The sample is then air dried, placed with a Tesa tape and measured with a semiconductor detector. In the following figure several filters are shown with diameters of 21 mm and 38 mm. The dark colour appearing in the 21 mm filter is caused from the silver iodide when exposed to light.

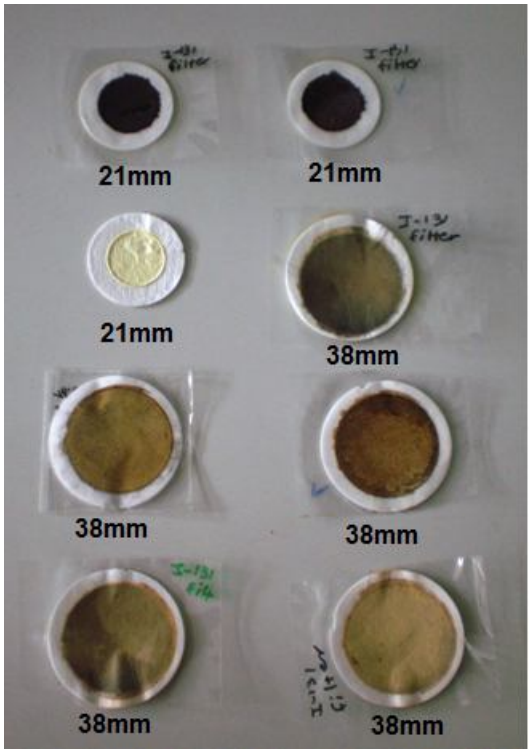

Figure 20: Measured silver iodide filters with diameters 21 mm and 38 mm.

2. Determination of the chemical yield of the method

The chemical yield was determined under experimental conditions with water samples of well known ^{131}I activities (WWTP outflow or Iodine pills diluted in river water). The task of estimating a reliable and consistent value of the chemical yield appeared to be rather difficult. The results are given in appendix 2. When performing the whole procedure the highest value of chemical yield that we were able to reach was close to 27% and with a second filtration 35%, values far from the 80-90% as Mundschenk reports. For this reason we decided to measure directly the 1st filter formed. Although Mundschenk's value was reached (89.6%), it was a high activity sample, a second filtration was done and the activity resulting was a combination of the filter activity and the precipitate. The procedure was repeated several more times under the same conditions, 1 filtration and measurement of the 1st filter. However the filtration time varied between 1-3 hours with no obvious reason and at the same time the results were not consistent. The value of the chemical yield was in a range of [20.7-62.0] %, although the procedure was conducted under the same conditions. These results let us

to the abandoning of the method and a more stable method for the determination of ^{131}I in the river water was carried out.

2.2 Gamma spectrometric method for determination of radionuclides in surface water

This method was also introduced by **Mundschenk, 1993** (Verfahren zur gamma-spektrometrischen Bestimmung von Radionukliden in Oberflächenwasser) and is a procedure for the determination of several isotopes in the surface water (^{137}Cs, ^{134}Cs, ^{131}I, ^{133}Ba, ^{54}Mn, ^{58}Co, ^{65}Zn, ^{88}Y, ^{109}Cd, ^{144}Ce). Since our interest is only ^{131}I we adjusted the method and at the same time simplified it.

The method is based on the precipitation of the target nuclides (^{131}I in our case) as insoluble compounds from large volumes with the addition of flocculants. The insoluble precipitates are formed by successive addition of pre-precipitation components in the initial sample, where colloidal AgI is bound to Bentonite particles which are themselves coagulated by a flocculant. The separated precipitate can be measured directly in either wet or dry form in a Marinelli beaker under defined counting conditions. A step by step complete description of the method follows.

1. Radiochemical separation

For a 20 litre river water sample the procedure is as follows:

1. A portion of the unfiltered sample of about 6 litres is poured into a plastic container (25 litres) and added 4 ml of potassium iodide solution (40 mg I^-) as a mixed solution. The iodide is added as an enhancer for the procedure.
2. We add 0.4 g of sodium sulphate (solid), as well as the remaining sample of 14 litres and stir to homogenize well.
3. Afterwards we add 4 ml of silver nitrate solution (40 mg Ag^+) and stir. The silver nitrate reacts with the potassium iodide according to the following reaction:
   $$KI + AgNO_3 \rightarrow KNO_3 + AgI \downarrow$$
   and gives colloid silver iodide.
4. Now, 24 g of disodium hydrogen phosphate ($Na_2HPO4 \circ 2H_2O$) is added under stirring conditions.
5. Then we add 160 ml Flygtol A (Bentonite) solution (3.2 g Bentonite- activated montmorillonite).
6. Subsequently, 40-60 ml of ammonia solution ($10 mol \cdot l^{-1}$) is added until we get an alkaline reaction (pH value > 8) and we keep stirring for 30 min.
7. After the stirring process is completed we add 80 ml Kerafloc solution (16 mg Kerafloc) (polyelectrolyte) and stir for about 3 min. The Kerafloc in combination with the bentonite are used to speed up the precipitation procedure.

8. We stop the stirring and let the sample precipitate overnight, in order to allow settling. In the following figure the precipitate in its original form is shown.

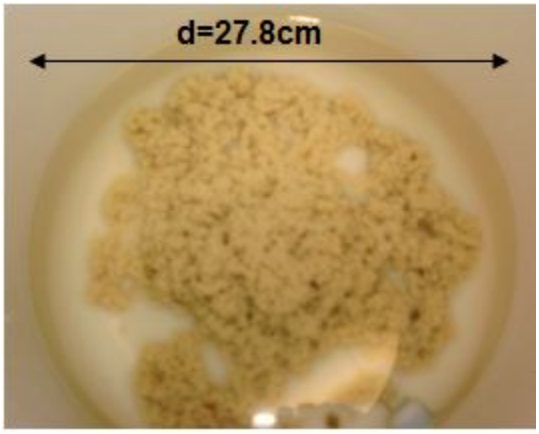

Figure 21: Silver iodide precipitate with the addition of bentonite and kerafloc.

9. After the precipitation occurs, the supernatant is siphoned or drawn off and discarded. The precipitate is poured into a Marinelli beaker and measured in wet state.

In order to avoid efficiency errors, because of precipitation inside the Marinelli beaker, wallpaper paste (glue) is added to the sample to make it homogeneous as shown in the next figure:

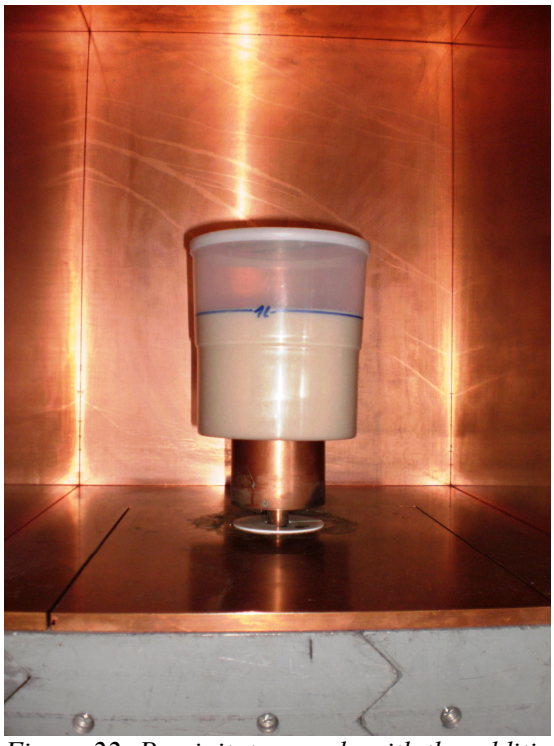

Figure 22: Precipitate sample with the addition of glue inside the detector.

In order to investigate the source of additional to ^{131}I isotopes appearing in our final sample, we measured samples of bentonite and glue (appendix 7). The spectra justified the presence of ^{214}Pb, ^{212}Pb, ^{208}Tl, ^{214}Bi and ^{40}K in our final spectrum. As expected, no ^{131}I was present in any of the additional spectra.

2. Determination of the chemical yield of the method

The chemical yield was determined under experimental conditions with water samples of well known ^{131}I activities (WWTP outflow). More than 10 different chemical extractions were performed with 20 Liters WWTP effluent each. The value of the chemical yield was in the range [39.6-66.3] %. However since the equipment was changed and bottles with an attached tap for decanting off the water were used, for the determination of the chemical yield only these values were taken under consideration, although it represented only 3 procedures, it was considered sufficient for the framework of this study.

The value of the chemical yield was determined: n= (63.3±8.3) %.

Possible losses of material, that would lead to this value and not closer to 100%, can be considered the attachment to the walls of the containers, to the transfer beakers, or to the equipment used, such as the stirrer. The following figure illustrates some possible loses of ^{131}I:

Figure 23: Left picture: 25 Liter container, Center picture: Material attached on the stirrer, Right picture: Material attached in beaker walls after the addition of glue and the transfer into a Marinelli beaker.

However these losses are believed to be a minor fraction, while the main loss is believed to originate from material remaining into the solution. Trace experiments with radioiodine in water samples have shown a conversion of ^{131}I into an iodine compound that cannot be precipitated as silver iodide by a silver nitrate solution **(Reifenhäuser C. and Heumann K., 1990).** Measurements of the water after the precipitation took place, were performed, however no ^{131}I was found above detection limit. Additional information can be found in appendix 2.

2.3 Calculation of the analytical results

With the gamma spectrometric determination of ^{131}I in water sample with volume V and chemical yield n, the activity concentration $c_{I\text{-}131}$ can be calculated using the following equation **(Mundschenk 1993**):

$$c_{I-131}(t_m) = \frac{R}{\varepsilon \cdot f \cdot n \cdot V} \cdot \frac{\lambda \cdot t_m}{1 - e^{-\lambda \cdot t_m}} = \frac{A}{n \cdot V} \cdot \frac{\lambda \cdot t_m}{1 - e^{-\lambda \cdot t_m}} \text{ [Bq l}^{-1}\text{]} \qquad (1)$$

where

R	the peak count rate of ^{131}I,
ε	the peak counting efficiency at 364.4 keV,
f	the emission frequency for ^{131}I,
λ	the decay constant of ^{131}I,
A	the activity and
t_m	the measurement time of the sample.

Here the beginning of the measurement has always to be selected as the reference time point t_m.
To convert the concentration of activity on the time of the sampling t_p, equation (1) should be adjusted accordingly:

$$c_{I-131}(t_p) = \frac{R \cdot e^{\lambda(t_m - t_p)}}{\varepsilon \cdot f \cdot n \cdot V} \cdot \frac{\lambda \cdot t_m}{1 - e^{-\lambda \cdot t_m}} \text{ [Bq l}^{-1}\text{]} \qquad (2)$$

The case of a gamma spectrometric determination of ^{131}I arises statistic counting errors s (s^{-1}) of the peak counting rate R (s^{-1}) can be calculated from the mean background counting rate per channel $\overline{R_o}$ (s^{-1}), the Full Width Half Maximum (FWHM) h (number of channels) and the measuring time t_m (s) as follows **(Mundschenk, 1993):**

$$s = \sqrt{\frac{R + 2 \cdot 1.7 \cdot h \cdot \overline{R_o}}{t_m}} \text{ [s}^{-1}\text{]} \quad (3)$$

Since the process can be approximated by peaks in a good approximation by a normal distribution, as evaluable peak area of the spectrum section we define the area which covers 95% of the entire peak area corresponding to 1.7h (2σ). Thus one receives the statistic counting error $s(c_{I-131})$ of ^{131}I determined by:

$$s(c_{I-131}) = \frac{s}{\varepsilon \cdot f \cdot n \cdot V} = c_{I-131} \cdot \frac{s}{R} \text{ [Bq l}^{-1}\text{]} \quad (4)$$

Or the relative standard deviation $s(c_{I-131})/c_{I-131}$ (variation coefficient):

$$\frac{s(c_{I-131})}{c_{I-131}} = \frac{s}{\varepsilon \cdot f \cdot n \cdot V \cdot c_{I-131}} = \frac{s}{R} \text{ [Bq l}^{-1}\text{]} \quad (5)$$

In our case, the Genie software, using the weight and efficiency of the sample as inputs, calculates the activity concentration and its error of our samples depending on the input parameter of the time, which we define as the date and time of sampling. Afterwards another calculation, manual this time, is performed to include the chemical yield factor and obtain the real activity concentration of our samples. All manual calculations are made according to the appendix 8.

Chapter 3

Sampling campaigns and results

For the purposes of this study 4 different sampling campaigns were performed. In all of them several factors had to be taken under consideration. All sampling locations were chosen in agreement to locations of existing sediment data for the best possible comparison. The maps were created by the GeoIQ platform in geocommons.com

3.1 1st sampling campaign

The 1st sampling campaign took place at 21st of June 2012. Samples were collected from 10 different locations along the river and covered a distance of approximately 18 km. The first sample was taken from the Bremen Karl-Carstens-Brücke and the last one close to Bremen-Vegesack. The samples were collected with a 10 liter bucket from the center on the river while on board to a river boat with an approximate location error of 500m (mean speed of boat close to 5m/s). The map below gives information on the sampling locations as well as the locations of the hydrological stations, the WWTP and sediment data.

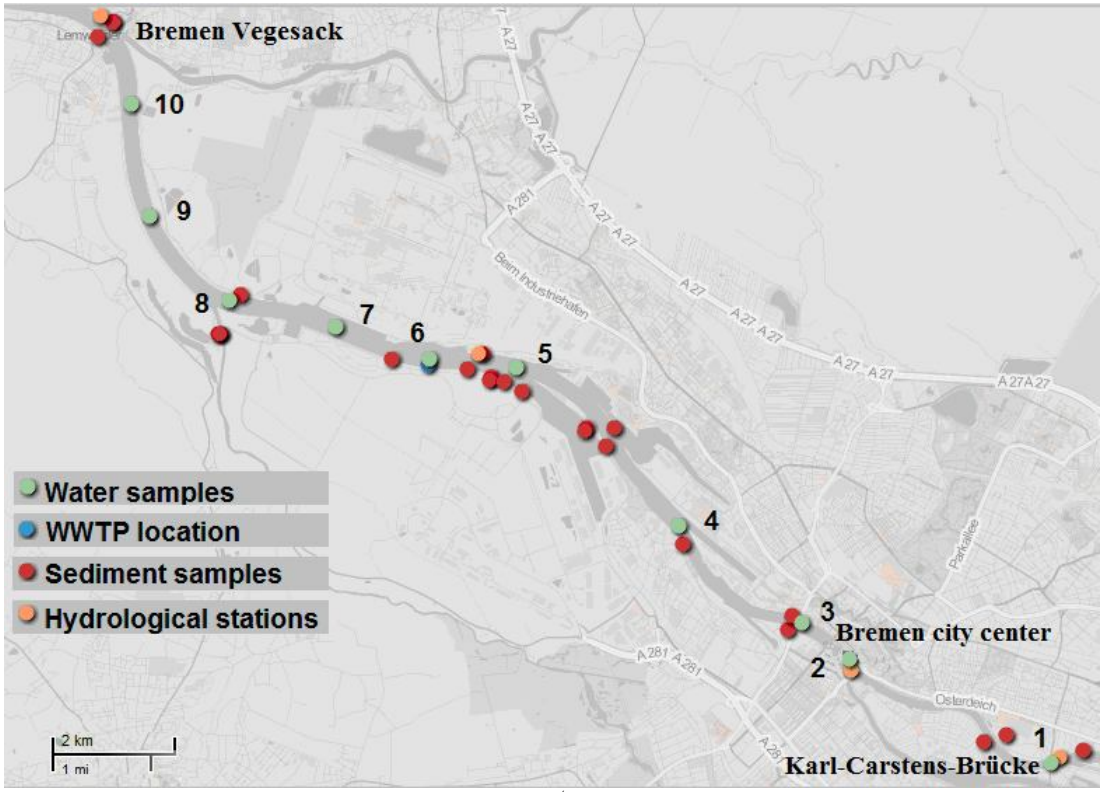

Figure 24: Water sampling locations of the 1st campaign, WWTP and Hydrological stations and sediment sampling locations.

All samples were analyzed in the same week to avoid additional decay loses and were measured close to 24 hrs each. The results are given in the next table (additional information about the samples is given in the appendix 3):

Table 4: Results from 1st sampling campaign.

Sample number	Geographical Coordinates	Activity concentration[mBq/kg]
1	N 53.05942 E 8.5262	< 2.6
2	N 53.0746848 E 8.8033550	< 3.9
3	N 53.0800513 E 8.7916655	< 3.4
4	N 53.0943026 E 8.7613274	< 4.6
5	N 53.1176365 E 8.7217211	< 4.7
6	N 53.1189690 E 8.7004711	< 6.5
7	N 53.1237193 E 8.6773089	< 5.1
8	N 53.1274369 E 8.6512045	< 5.5
9	N 53.1399654 E 8.6318358	< 4.9
10	N 53.1563479 E 8.6271664	< 4.0

All the activities measured were under detection limit. The sampling timing could have been a crucial factor to this result, since the samples were collected between high and low tide with a maximum flow velocity towards the coast. Also the meteorological conditions (heavy precipitation) occurring to the south of Bremen, affecting the catchment area of the Weser River, may have contributed to enhanced river flow resulting to enhanced dilution of the ^{131}I activity of the WWTP. According to the formula **(Fischer H. et al, 2009):**

$$C_{river} = C_w \cdot Q_{WWTP} \cdot Q_{river}^{-1} \qquad (\alpha)$$

where

C_{river}: concentration of the isotope in river water

C_w: concentration of the isotope in WWTP water

Q_{WWTP}: mean discharge of the WWTP

Q_{river}^{-1}: mean discharge of the river

and considering the fact that the WWTP discharge at the given date had a mean value of 0.99m^3/s till the time of sampling (appendix 5) and the mean river discharge is 330m^3/s **(Rijn L., 2011)** the mean activity concentration in WWTP discharge water 234 mBq/l (appendix 4) after complete dilution the concentration of the isotope in river water becomes 0.7 mBq/l, value lower than the detection limit.

Thus, in an attempt to located the regions of interest we use a simple equilibrium model as presented in **Fischer H. et al, 2009,** which is based on German regulations **(AVV, 1990)** and we calculate the expected activity concentration in the water from known sediment activity concentrations from S.Ulbrich, 2008 and P.Lysogne, 2009 master thesis (appendix 1).

In order to calculate the activity concentration in the water we need to calculate the sediment deposition density and the activity concentration of the isotope in suspended matter. For these calculations we use the formulas below, as described from the equilibrium model:

(i) $a = \frac{O}{d \cdot \rho} \rightarrow O = \alpha \cdot d \cdot \rho$, (β)

where
O is the sediment deposition density,
α is the activity concentration of the sediment,
d is the thickness of the sampled sediment layer (d=5mm) and
ρ is the sediment density (ρ=700 kgm^{-3}).

(ii) $O = \frac{\rho_s \cdot v_s \cdot C_{sm}}{\lambda_r}\left(1 - e^{-\lambda_r \cdot t_s}\right) \rightarrow C_{sm} = \frac{O \cdot \lambda_r}{\rho \cdot v}\left(1 - e^{\lambda_r \cdot t_s}\right)^{-1}$, (γ)

where:
C_{sm} is the activity concentration of the isotope in suspended matter
v_s is the sedimentation growth rate ($v_s=2.1 \cdot 10^{-10}$ $m \cdot s^{-1}$)
λ_r is the radioactive decay constant ($\lambda_r=10^{-6} s^{-1}$) and
t_s the time allowed for sedimentation ($t_s=2.6 \cdot 10^{6}$s, value equal to one month when the equilibrium is almost reached).

And (iii) $C_{sm}=K_F \cdot C_w \rightarrow C_w = \frac{C_{sm}}{K_F}$, (δ)

where:
K_F is the concentration factor ($K_F=10^4$ $L \cdot kg^{-1}$) and
C_w is the concentration of isotope in the water.

The calculation results for the expected water activity concentration and its error for P.Lysogne and S.Ulbrich data are given in the tables below, distances indicated with negative sign are in the direction towards the city center while the rest in the direction towards the coast:

Table 5: P.Lysogne sediment data- expected water activity

Distance from WWTP (km)	Activity concentration of sediment (Bq/kg[DM])	Expected activity concentration in river water (mBq/l)
-12.2	0.5±0.1	1.2±0.1
-11	0.3±0.1	0.8±0.1
-10.5	0.7±0.3	1.9±0.6
-4.5	0.5±0.6	1.3±0.4
-1.5	6.5±0.3	16.8±0.7
-0.55	9.2±0.6	45.4±1.4
0	46.8±1.8	120.4±4.6
1.5	27.7±1.1	71.3±2.8
3	9.6±0.9	24.7±2.4
5	3.8±0.1	9.9±0.1
10	1.2±0.1	3.1±0.3
12	1.3±0.2	3.4±0.6
14	1.3±0.1	3.3±0.3
17.4	0.4±0.1	1.0±0.3
24	0.6±0.1	1.5±0.4

Table 6: S.Ulbrich sediment data-expected water activity

Distance from WWTP (km)	Activity concentration of sediment (Bq/kg[DM])	Expected activity concentration in river water (mBq/l)
- 6.5	1.9±0.2	4.9±0.4
- 6.5	1.6±0.3	4.1±0.7
- 4.5	2.3±0.4	6.0±1.0
- 2.5	1.8±0.3	4.6±0.7
- 2.25	1.5±0.4	3.9±1.0
- 2	2.5±0.9	6.6±2.2
0	122.3±3.1	314.8±8.0
0.5	1.8±0.5	4.5±1.2
1.75	3.7±0.2	9.6±0.5
4.5	2.7±0.3	7.0±0.7
5	0.5±0.2	1.2±0.5
9.75	0.7±0.1	1.9±0.2
9.75	0.6±0.1	1.6±0.3
12.75	0.7±0.1	1.7±0.2
14	0.8±0.1	1.9±0.2
17.5	0.8±0.1	2.2±0.3
20	0.5±0.1	1.2±0.1

The calculations through this simple equilibrium model indicate that only in distances up to 1.5 km upstream and 6.5 km downstream to the WWTP we will be able to obtain samples with activity concentration in the water above detection limit.

3.2 2nd sampling campaign

The second sampling campaign took place in the 3rd of July 2012. Only two samples we collected and we both analyzed the day after the sampling. Along with the water samples, WWTP effluent was collected. The location of the samples is shown in the figure below:

Figure 25: Sampling location 11 and 12 (the location corresponds to point 6 in Figure 24).

The activity concentrations of the collected samples are given in the following table.

Table 7: Results from 2nd sampling campaign.

Sample number	Geographical Coordinates	Activity concentration[mBq/kg]
WWTP outflow	N 53.114956 E 8.714502	121.1±12.3
11	N 53.11641 E 8.71525	96.4±13.7
12	N 53.11635 E 8.71559	95.2±13.3

The activity concentrations of samples 11 and 12 did not differ, which indicates that the WWTP outflow activity is homogeneous. However there is a significant reduction, close to 20.9% for a short distance (approximately 170m) from the WWTP effluent location and the boundary between the outflow and the main river.

Additional to the water samples, 2 sediment samples were collected in this location with activity concentration 26.9±1.0 and 26.9±1.4 Bk/kg[DM]. More information can be found in appendix 1.

3.3 3rd and 4th sampling campaigns

In order to investigate the widest area affected by WWTP emissions, we performed two more sampling campaigns. During the 3rd campaign samples were collected in the locations 13-16, between low and high tide where the flow velocity was medium and had a direction towards the city center. The opposite conditions were present during the 4th sampling campaign in which samples in the locations 17-20 were collected, medium flow velocity with direction to the coast. Along with the river water samples, WWTP effluent was collected for both campaigns. Schematically the sampling locations are given in the figure below:

Figure 26: Sampling locations for campaigns 3rd and 4th.

In only one sample upstream (sample #13) activity was found above detection limit and in three samples downstream (samples #17, 18 and 19). More specifically the activity results are given in the following table:

Table 8: Results from 3rd and 4th sampling campaigns.

Sample number	Geographical Coordinates	Activity concentration[mBq/kg]
13	N 53.116086 E 8.717206	21.9±1.8
14	N 53.1145 E 8.722436	< 3.5
15	N 53.111506 E 8.727997	< 3.7
16	N 53.108719 E 8.731219	< 4.2
17	N 53.116572 E 8.7148	50.3±7.6
18	N 53.117481 E 8.707653	7.9±2.5
19	N 53.117533 E 8.701722	5.7±2.6
20	N 53.117567 E 8.695825	< 4.1

3.4 ^{131}I profile along Weser River

The ^{131}I water activity concentration results were used to create a profile of the isotope along the river, in comparison with the sediment activity concentration as shown in the next figure:

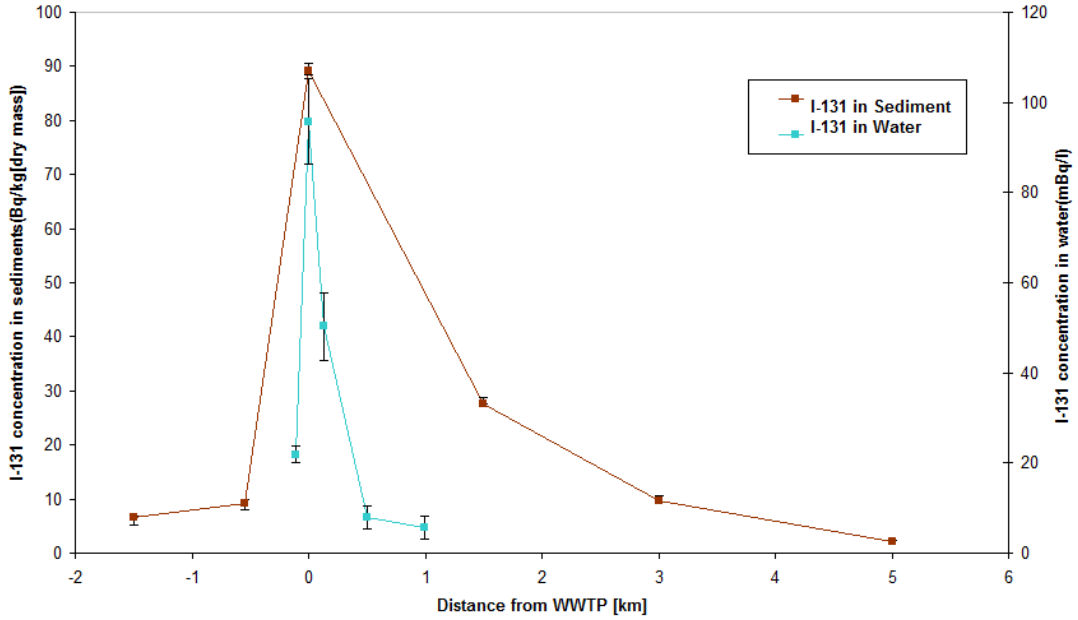

Figure 27: ^{131}I profile in Weser River (positive values of distance indicate the direction towards the coast and negative towards the Bremen city center, lines are included for better visibitily, Sediment data: S.Ulbrich master thesis 2008, P. Lysogne master thesis 2009, Water data: this work)

The profiles correspond to each other. Both curves show a peak of highest activity in the WWTP which decreases the further we go, reaching a plateau when activities are below detection limit. The asymmetry in activity between upstream and downstream measurements is obvious, not only as a difference in activity concentration values but also upstream the detection limit is reached in shorter distance from the WWTP compared to downstream, both for sediments and water.

In order to quantify these differences, WWTP water was collected along with each sampling campaign. As mentioned before between the WWTP activity concentration in the effluent and in the boundary to the river (2nd sampling campaign) there was a reduction of 20.9%. Comparing the activity concentration of the effluent and a sample collected upstream (3rd sampling campaign- sample 13) with a distance of approximately 280m we observe a reduction close to 90%, while for the same distance but downstream (4th sampling campaign- sample 17) we have a reduction of 79% and close to 1 km even further downstream (sample 19) we have a reduction of 97.6%.

Chapter 4

Model describing the ^{131}I transport in river water

Several mathematical models of different degrees of perfection exist for simulating the transport of radioactive substances by a uniform flow in one, two or three dimensions. The most important processes influencing the behavior of radionuclides are shown in the following figure and include adsorption, desorption, sedimentation of suspended particles, scour and resuspension from the active sediment layer, and radioactive decay for the radionuclide, particulate adsorbed radionuclide and activity transfer between the pore water of the bed and overlying water.

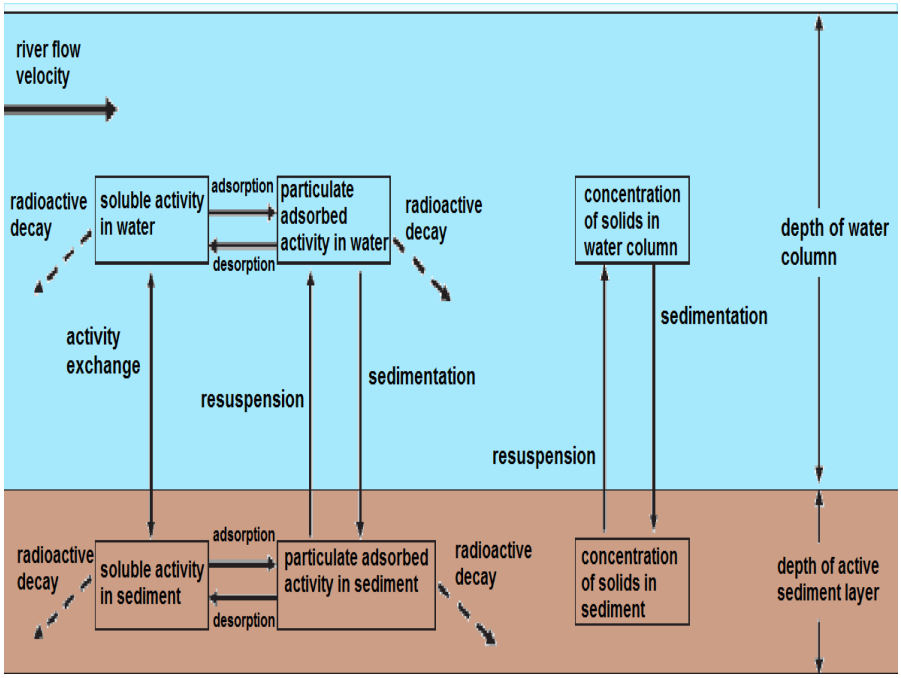

Figure 28: Schematic of reactions in the river water column and sediment. **(Schnoor J., 1996)**

The six compartment model can be reduced to a system of 2 differential equations by making the following assumptions **(Schnoor J., 1996):**

- the total concentration in the water column and in the bed sediment is the sum of the soluble and particulate adsorbed radionuclide
- instantaneous equilibrium between adsorption and desorption
- under the assumption of instantaneous equilibrium, the amount of radionuclide that is sorbed to the bottom sediments can be related to the dissolved radionuclide concentration using a linear adsorption isotherm
- steady state condition for solids concentration in bed
- constant velocities in longitudinal and lateral directions
- constant dispersion coefficients

The first equation (I) describes the transport of activity in the river water and the second equation (II) describes the activity concentration in the sediments:

$$\frac{\partial C}{\partial t} = \underbrace{-u\frac{\partial C}{\partial x}}_{\text{advection x-direction}} + \underbrace{E_x\frac{\partial^2 C}{\partial x^2}}_{\text{dispersion x-direction}} \underbrace{-v\frac{\partial C}{\partial y}}_{\text{advection y-direction}} + \underbrace{E_y\frac{\partial^2 C}{\partial y^2}}_{\text{dispersion y-direction}} \underbrace{-\lambda\frac{C}{(1+k_{PW}S_W)}}_{\text{radioactive decay}} \underbrace{-k_s\left(\frac{k_{PW}S_w}{1+k_{pw}S_w}\right)C}_{\text{sedimentation}} +$$

$$\underbrace{+\frac{k_L}{d}\left(\frac{r}{k_{Pb}} - \frac{C}{1+k_{PW}S_W}\right)}_{\text{pore-water diffusion}} \underbrace{+\alpha\frac{S_b r}{\gamma}}_{\text{resuspension}} \quad \text{(I)}$$

$$\frac{\partial r}{\partial t} = \underbrace{-\lambda\frac{r}{(1+k_{Pb}S_b)}}_{\text{radioactive decay}} \underbrace{+\frac{k_s k_{PW} S_w \gamma}{\left(S_b + \frac{1}{k_{Pb}}\right)}C}_{\text{sedimentation}} \underbrace{-\alpha\frac{S_b}{\left(S_b + \frac{1}{k_{Pb}}\right)}r}_{\text{resuspension}} -$$

$$\underbrace{-\frac{k_L}{d\left(S_b + \frac{1}{k_{Pb}}\right)}\left[\frac{r}{k_{Pb}} - \frac{C}{1+k_{PW}S_W}\right]}_{\text{pore-water diffusion}} \quad \text{(II)}$$

where

C: total concentration activity in the water column (Bq/l)
x: longitudinal (downstream) distance (m)
u: longitudinal (downstream) velocity (u=0.30m/s, Hydrological data appendix 6)
E_x: longitudinal dispersion coefficient, range 10^{-1}-10^4 m^2/s **(EPA- Watershed& Water Quality Modeling Technical Support Center, 2012),** in our case estimated 10 m^2/s.
y: lateral distance (m)
v: lateral velocity (v =$6.3\cdot10^{-3}ms^{-1}$, calculated as mean discharge from WWTP, 1.3 m^3/s (appendix 5) / cross sectional area of WWTP effluent= width (39.2 m) *depth (5.3 m) , **Rijn L., 2011**)
E_y: lateral dispersion coefficient, range 10^{-2}-10^0 m^2/s **(EPA- Watershed& Water Quality Modeling Technical Support Center, 2012),** in our case estimated 0.48 m^2/s
λ: radioactive decay constant for ^{131}I is $\lambda=10^{-6}s^{-1}$
k_{PW}: distribution (partition) coefficient in water column, k_{PW} = 10 l/kg **(Punt A., et al., 2007)**
S_W: solids concentration in the water column, S_W = 10 kg/l **(Semizhon T. et al., 2010)**

k_s: sedimentation rate constant (v_w/h, mean particle settling velocity **(Semizhon T. et al., 2010, Huijts K. et al., 2006)** / mean depth of Weser River **(Rijn L., 2001)** = [10^{-3}-10^{-5}] ms^{-1}/ 5.3m≈[10^{-4}-10^{-6}] s^{-1}), in our case estimated as $10^{-4}s^{-1}$
k_L: mass transfer coefficient between water column and pore water of bed sediment, range 10^{-5}-$10^{-8}ms^{-1}$ **(Semizhon T. et al., 2010)** , in our case estimated 10^{-5} ms^{-1}
d: depth of active bed sediment (sedimentation growth rate $v_s \cdot$ time and with $v_s = 2.1x10^{-10}$ ms^{-1} **(Fischer H. et al., 2009)** and assuming that after 10 half lives all the ^{131}I will have decayed, the exchange layer thickness is d= $1.5x10^{-3}$ m)
r: amount of adsorbed radionuclide on sediment solids (Bq/kg[dry weight])
k_{Pb}: distribution (partition) coefficient in sediment, sediment $k_{Pb} = 10^4$ l/kg **(Fischer H. et al, 2009)**
α: scour/ resuspension rate constant (mass exchange coefficient due to stirring up **(Krylov A. et al., 2006, Semizhon T. et al., 2010)** / exchange layer thickness = 10^{-8} -$10^{-9}ms^{-1}$/$1.5\cdot10^{-3}$m≈10^{-5}-$10^{-6}s^{-1}$), in our case estimated $6.5\cdot10^{-6}$ s^{-1}
S_b: solids concentration in the bed, S_b = 2650 kg/l **(Huijts K. et al., 2006)**
γ: ratio of water depth of Weser River h=5.3m **(Rijn L., 2001)** to depth of active bed sediment d= $1.5x10^{-3}$ m, $\gamma=3.5\cdot10^3$m).

The first two terms of equation (I), describe the advection dispersion transport of the radionuclide in the case of constant velocity and constant dispersion coefficient. The remaining terms describe the same processes in both equation (I) and (II). Radioactive decay occurs via first order radioactive decay constant λ . First order process is also the sedimentation of the radionuclide which occurs via first order sedimentation rate constant k_s. Pore- water diffusion is based on the concentration difference between the pore water and the overlying water. The resuspension from the bed sediment to the overlying water is described by using a first order coefficient α.

4.1 Analytical solution for the 2 dimensional advection-dispersion equation with decay term

Considering the above equations, several terms can be neglected since the processes which describe have a much smaller time scales than the water flow. Especially in the region we want to investigate (up to 5 km downstream and 1 km upstream) with longitudinal river velocity of u= 0.30 m/s (Hydrological data appendix 6) the time require to cover this distance is less than 4 hours and slow processes can be omitted from our equation.

More precisely, for each term of the equation (I) with the values given above:

Radioactive decay term: $\frac{\lambda}{1+k_{PW}\cdot S_W} = \frac{10^{-6}}{1+10\cdot10^{-5}} \approx 10^{-6}$ s^{-1}

Sedimentation term: $\frac{k_s \cdot k_{PW} \cdot S_W}{1 + k_{PW} \cdot S_W} = \frac{10^{-4} \cdot 10 \cdot 10^{-5}}{1 + 10 \cdot 10^{-5}} \approx 10^{-8}$ s^{-1}

Mass transfer from the pore water of bed sediment to the water column:

$$\frac{k_L}{d \cdot k_{Pb}} = \frac{10^{-5}}{1.5 \cdot 10^{-3} \cdot 10^{4}} = 6.67 \cdot 10^{-7} \frac{kg}{s \cdot l}$$

Mass transfer from the water column to the pore water of bed sediment:

$$\frac{k_L}{d \cdot (1 + k_{PW} \cdot S_W)} = \frac{10^{-5}}{1.5 \cdot 10^{-3} \cdot (1 + 10 \cdot 10^{-5})} = 6.66 \cdot 10^{-3} \text{ s}^{-1}$$

Resuspension from the bed sediment to the water column:

$$\frac{a \cdot S_b}{\gamma} = \frac{[10^{-5} - 10^{-6}] \cdot 2.65}{3.5 \cdot 10^{3}} \approx [10^{-8} - 10^{-9}] \frac{kg}{s \cdot l}$$

The mass transfer from the water column to the pore water of bed sediment dominates the rest of the terms by a factor of 1000, which allows us to neglect them in a 1st approximation.

With these simplifications the 2 dimensional advection dispersion equation for river flow with decay, describing the sedimentation process is:

$$\frac{\partial C}{\partial t} = -u \frac{\partial C}{\partial x} - v \frac{\partial C}{\partial y} + E_x \frac{\partial^2 C}{\partial x^2} + E_y \frac{\partial^2 C}{\partial y^2} - k \cdot C, \qquad \text{where } k = \frac{k_L}{d \cdot (1 + k_{PW} \cdot S_W)}$$

In order to estimate the importance of each term, we use the scales presented in the next table along with the Peclet number.

Table 9: Scaling of variables.

Variable	Scale	Choice of value
C	C	Typical concentration value
u	U	Typical velocity value
x	L	Approximate domain length

Peclet number: $Pe = \frac{advection}{dispersion} = \frac{UC/L}{EC/L^2} = \frac{UL}{E}$

If Pe<<1 the advection term is significantly smaller than the dispersion term then the dispersion dominates while the advection is negligible. If Pe>>1 the advection term is significantly larger than the dispersion term then the advection dominates while the dispersion is negligible and the spreading is almost inexistent. If Pe~1, the advection and dispersion terms are not significantly different and neither process dominates over the other.

We are interested in investigating a region close to the bank of the river (y < 2 m) for a distance from the source up to 5 km downstream. In the lateral direction the advection term is rather small compared to the dispersion term giving a Peclet number

of $Pe = \frac{vL}{E_y} = \frac{6.3 \cdot 10^{-3} ms^{-1} \cdot 2m}{0.48 m^2 s^{-1}} = 0.026 << 1$ and as a result the advection can be neglected. In the longitudinal direction the opposite appears to be true. High flow velocity leads to high Peclet number of $Pe = \frac{uL}{E_x} = \frac{0.3 ms^{-1} \cdot 5000m}{10 m^2 s^{-1}} = 150 >> 1$ and as a result the advection dominates over dispersion in the longitudinal direction.

Taking under consideration the scaling, the equation becomes:

$\frac{\partial C}{\partial t} = -u\frac{\partial C}{\partial x} + E_y \frac{\partial^2 C}{\partial y^2} - kC$, with $k = \frac{k_L}{d \cdot (1 + k_{PW}.S_W)}$ the effective decay term.

In our case we have approximately constant inflow of radioactive iodine, which leads to steady state conditions $\left(\frac{\partial C}{\partial t} = 0\right)$:

$$u\frac{\partial C}{\partial x} = E_y \frac{\partial^2 C}{\partial y^2} - kC$$

We look for an exponential solution of the form: $C(x,y) \prec e^{\lambda(x+y)}$ and by substituting in the above equation we get:

$$E_y \lambda^2 - u\lambda - k = 0$$

which is a homogeneous equation of quadratic form with:

$$\lambda_{1,2} = \frac{u \pm \sqrt{u^2 + 4E_y k}}{2E_y}$$

Our solution becomes:

$$C(x,y) = C(0,0)e^{\lambda_{1,2}(x+y)}$$

In our case we are interested in the left bank of the river where we collected our samples, so for y=0 and C_0=C(0,0) the activity concentration at the location of inflow x=0, the solution becomes:

$C(x) = C(x,0) = C_0 e^{\lambda_1 x}$ for x≤ 0
and
$C(x) = C(x,0) = C_0 e^{\lambda_2 x}$ for x≥0.

At the same time by substituting the activity concentration in the water in equation (II) and solving it in terms of the activity concentration in sediments, keeping the radioactive decay term and assuming a steady state situation ($\frac{\partial r}{\partial t} = 0$) we get:

$$r(x) = \frac{\dfrac{k_s \cdot k_{PW} \cdot S_W \cdot \gamma}{\left(S_b + \dfrac{1}{k_{Pb}}\right)} + \dfrac{k_L}{d \cdot \left(S_b + \dfrac{1}{k_{Pb}}\right) \cdot \left(1 + k_{PW} \cdot S_W\right)}}{\dfrac{\lambda}{1 + k_{Pb} \cdot S_b} + \dfrac{a \cdot S_b}{S_b + \dfrac{1}{k_{Pb}}} + \dfrac{k_L}{d \cdot k_{Pb} \cdot \left(S_b + \dfrac{1}{k_{Pb}}\right)}} \cdot C(x)$$

4.2 Model simulations

A literature survey allowed the estimation of the parameters used for the simulation of transportation of ^{131}I in Weser river water. The simulations were performed through Matlab and its code is given in appendix 9. The equations used are the ones described in the previous paragraph; however the tidal effect of Weser River was not taken into consideration since we "approximated" the tidal river by a non tidal one, with constant flow velocity. For a distance 500 m upstream and 2500 m downstream of the WWTP the activity concentration of ^{131}I in the water was determined, assuming as input in the river the value C(0,0)= 121 x 0.8 mBq/l (the factor 0.8 is used to express the loss of the activity from the WWTP effluent until the boundary with the river, which in our case is the source and the value 121 mBq/l was the activity concentration measured in the WWTP effluent during the 2nd campaign, see chapter 3.4). The rest of the parameters were set as:

Table 10: Model parameter values

Parameter	Value
E_y	0.48 $m^2 \cdot s^{-1}$
k_s	10^{-4} s^{-1}
λ	10^{-6} s^{-1}
S_W	10^{-5} $kg \cdot l^{-1}$
S_{Pb}	2.65 $kg \cdot l^{-1}$
k_{PW}	10 $l \cdot kg^{-1}$
k_{Pb}	10^4 $l \cdot kg^{-1}$
k_L	10^{-5} s^{-1}
α	$6.5 \cdot 10^{-6}$ s^{-1}
γ	$3.5 \cdot 10^5$
d	$1.5 \cdot 10^{-3}$ m

and we get:

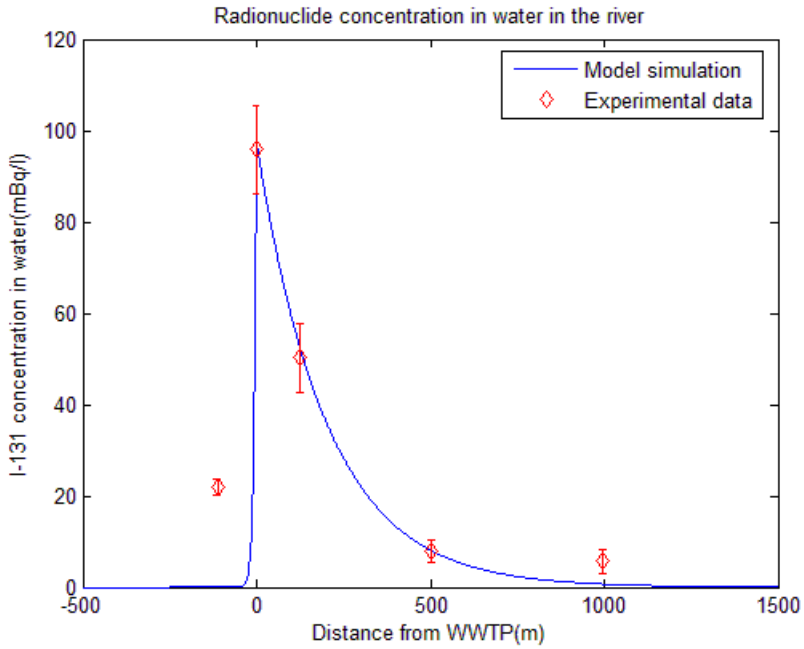

Figure 29: Activity concentration of ^{131}I in water along the river- model simulations and experimental data (E_y= 0.48 m^2s^{-1})

The comparison between simulation and experimental data for the ^{131}I activity concentration in the water shows good agreement. In the region upstream of the WWTP the model predicts almost zero ^{131}I activity concentration. This result could be expected, since as mentioned before, the Weser is a tidal river, fact which was not taken into account in the design of the model. By trying different values of the parameters, within the limits given in the literature we observe large variations of the modeling results. Especially the diffusion coefficient had a large impact on the width of the curve, even for small variations as shown in the next figure:

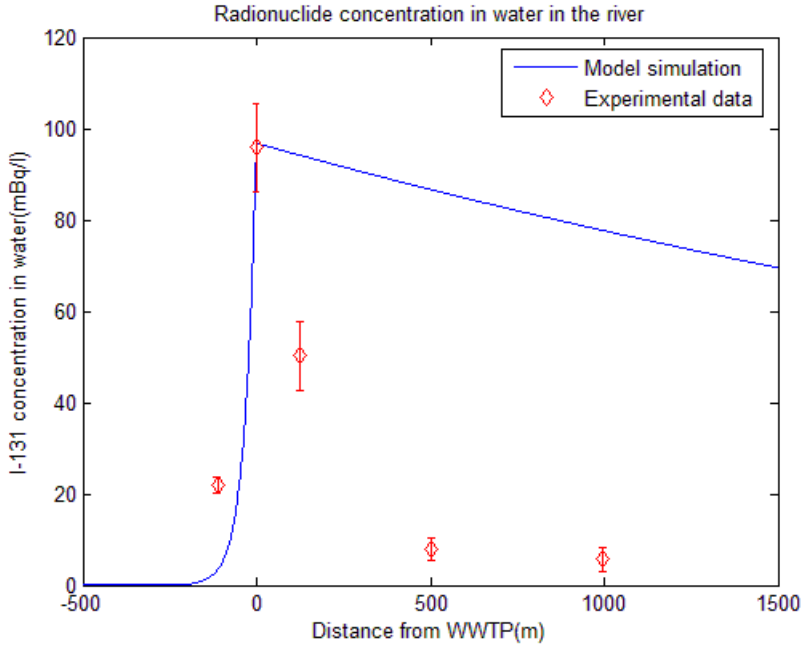

Figure 30: Activity concentration of ^{131}I in water along the river- model simulations and experimental data (E_y= 0.1 m^2s^{-1})

By using the model parameter values as given in table 10, the simulations for the activity concentration in sediments becomes:

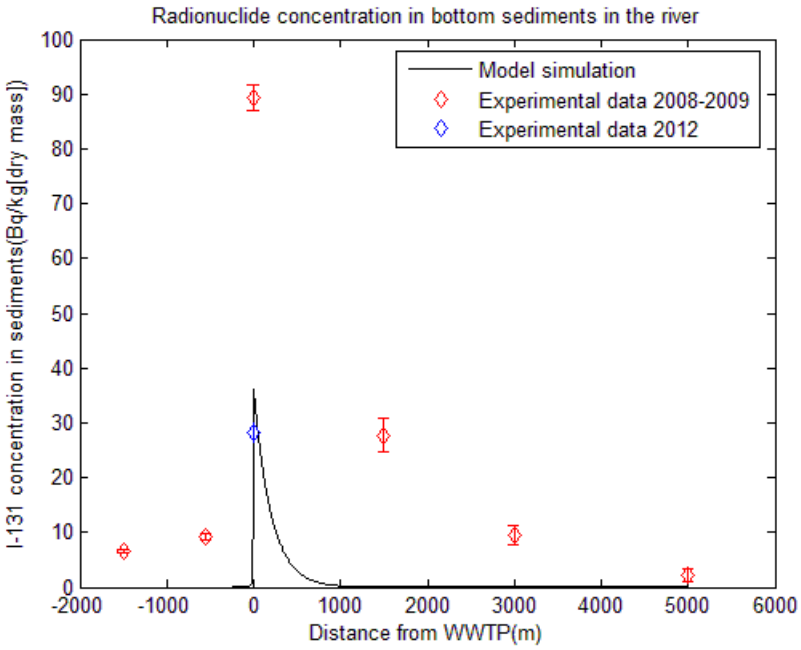

Figure 31: Activity concentration of ^{131}I in sediments along the river - model simulations and experimental data ($\alpha = 6.5 \cdot 10^{-6} s^{-1}$)

The simulation for the sediment does not agree with the experimental data of 2008-2009. The experimental data 2012 appears to fall in the simulation region. However since it is only one sampling site (right outside the WWTP) it is not sufficient to validate our model. Again large variations can be observed by slightly changing the value of parameters, more precisely by reducing the resuspension rate constant by a factor of 2.5 ($\alpha = 2.5 \cdot 10^{-6} s^{-1}$), we get:

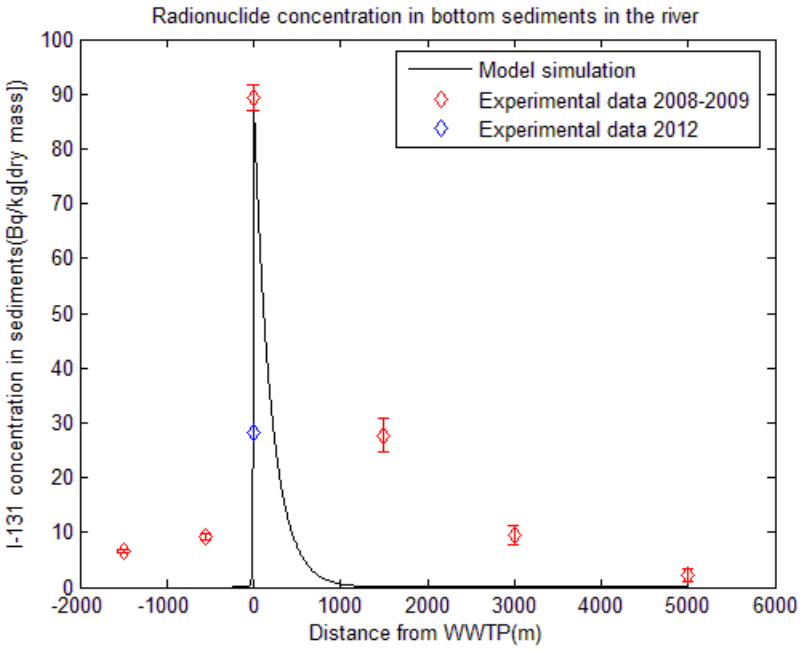

Figure 32: Activity concentration of ^{131}I in sediments along the river - model simulations and experimental data ($\alpha = 2.5 \cdot 10^{-6} s^{-1}$)

Although the model simulations seem to be in a good agreement to the activity concentration in the water, we cannot say the same for the activity concentration in sediments. After all the parameters used were mostly estimated through literature and may not have been applicable in our case. In general, the data we had available were limited and as a result the model cannot be properly assessed. Additional sampling is necessary for both water and sediments in order to determine if this model is capable of describing properly our experimental data.

Conclusions-Outlook

In this master thesis, the first step was done in the definition and testing of a proper ^{131}I chemical extraction method which is now used in other projects, although several difficulties came up, in which a considerable amount of time was devoted in order to be solved.

The fact that the 1st chemical extraction method proved not trustworthy in order to determine the ^{131}I in river water, lead us to the use of another one with higher detection limit. The 2nd chemical extraction method allowed us to reach more than 20 times lower detection limit than a direct measurement. Even so the detection limit was high enough not to allowing us to measure ^{131}I in river water in locations further than 1.5 km from the WWTP. The simple equilibrium model for estimating the activity concentration of ^{131}I in the river water was appeared useful in determining the areas of interest.

As expected we find the highest activity concentration values close to the WWTP outflow. Even for short distances and with imperfect mixing with river water we find substantial (more than 20%) reduction of radioactive material.

This lack of data created a secondary effect. The model created in order to describe the transport of ^{131}I in river water and sediments could not be properly assessed.

However there are improvements that can be made. First of all in the method we used. The chemical yield as mentioned before was determined from a few test measurements with WWTP water. In order to be able to use this value (63.3±8.3) % in further studies, we need to repeat the procedures and obtain a statistical significant result. Apart from that, we could try to lower the detection limit even more, by centrifuging the precipitate and measuring it in a Petri dish, geometry that would allow us to reach more than 2 times lower detection limit. Lower detection limit could also be reached by increasing the volume of our samples; however the sampling procedure would become more difficult.

References

1. **Audi G., et al**., *The NUBASE evaluation of nuclear and decay properties*, Nuclear Physics A, Volume 624, Issue 1, Pages 1-124, **1997**.
2. **AVV, 1990**. Allgemeine Verwaltungsvorschrift zu x45 Strahlenschutzverordnung: Ermittlung der Strahlenexposition durch die Ableitung radioaktiver Stoffe aus kerntechnischen Anlagen oder Einrichtungen. Bundesanzeiger 42 (64a), 1–23 (in German).
3. **Barquero R., et al**., *Liquid discharges from patients undergoing ^{131}I treatments*, Journal of Environmental Radioactivity, Volume 99, Issue 10, Pages 1530-1534,**2008**.
4. **Barquero R., et al**., *Liquid discharges from the use of radionuclides in medicine (diagnosis)*, Journal of Environmental Radioactivity, Volume 99, Issue 10, Pages 1535-1538, **2008**.
5. **Begleitforschung** §17b Abs8 KHG Datenjahr 2009.mde, www.g-drg.de, **2012**
6. **Canberra Industries**: Basic Counting System, http://www.canberra.com/pdf/Products/Basic-Counting-System.pdf, **2010**
7. **Canberra Industries**: Spectrum Analysis, http://www.canberra.com/pdf/Products/Spectrum-Analysis.pdf, **2010**
8. **Covidien Pharmaceuticals**: http://pharmaceuticals.covidien.com/pharmaceuticals/pagebuilder.aspx?topicID=132420&page=print, **2012**
9. **Debertin K. and Helmer R**., "Gamma and X-ray spectrometry with semiconductor detectors", Elsevier Science Publishers, **1988**
10. **Department of Chemistry, Washington University in St. Louis**: http://www.chemistry.wustl.edu/~edudev/LabTutorials/PeriodicProperties/MetalBonding/MetalBonding.html, **2002**
11. **EPA Method 902.0**, *Radioactive Iodine in drinking water.*
12. **EPA Watershed & Water Quality Modeling Technical Support Center**: www.epa.gov/athens/wwqtsc/courses/wasp7/transport/Dispersion.ppt, **2012**
13. **Fischer H, et. al**., *Medical radioisotopes in the environment-following the pathway from patient to river sediment*, Journal of Environmental Radioactivity, Volume 100, Issue 12, Pages 1079-1085, **2009**.
14. **Fischer H.,** *Radioisotopes in soil*: http://www.pep.uni-bremen.de/services/lectures/practicals/meas_tech_radioactivity_hf_rev3.pdf, **2003**
15. **Formation Evaluation Society of Australia**: http://www.fesaus.org/glossary/doku.php?id=terms:welcome, **2010**
16. **Gilmore G.,** "Practical Gamma-ray spectrometry", John Wiley and Sons, **2008**
17**. Homepage wissenschaftlicher Themen**: http://www.hpwt.de/Kern2e.htm, **2002**
18. **Huijts K.,** *Lateral entrapment of sediment in tidal estuaries: An idealized model study*, Journal of Geophysical Research, Lolume 111, C12016, **2006**.
19. **Isotope library:** http://ie.lbl.gov/toi/nucSearch.asp, **2004**
20. **Jardin C., et al**., Inside radiology: http://www.insideradiology.com.au/PDF/T44Ciodine131-consumer.pdf, **2009**
21. **Knoll G.,** "Radiation detection and measurement", John Wiley and Sons, **2000**
22. **Krylov A., et al.,** *Assessment of Concentration of Radionuclides in River Water and Bottom Sediments*, Russian Meteorology and Hydrology, Volume 32, Issue 7, Pages 470-478, **2007**.
23. **Lieser K.,** "Nuclear Radiochemistry: fundamental and applications", Wiley-VCH, **2001**

24. **Mundschenk H**., *Verfahren zur Bestimmung von Iod-131 in Oberflächenwasser*, C-I-131-OWASS-01, Leitstelle für Oberflächenwasser, Schwebstoff und Sediment in Binnengewässern, **1993**.
25. **Mundschenk H**., *Verfahren zur gammaspektrometrischen Bestimmung von Radionukliden in Oberflächenwasser,* C-γ-SPEKT-OWASS-01, Leitstelle für Oberflächenwasser, Schwebstoff und Sediment in Binnengewässern, 1**993**.
26. **Nakamura A., et al**., *Output of Radiopharmaceutical nuclides of known injected doses from a municipal sewage treatment system*, Health Physics, Volume 88, Issue 2, Pages 163-168, **2005.**
27. **Parekh P., et al**., *Rapid radiochemical analysis of ^{131}I in environmental samples using a well-type Ge-detector*, Journal of Radioanalytical and Nuclear Chemistry, **2003**.
28. **Punt A., et al.,** Environmental Agency: Radionuclide discharges to sewer-A field investigation, Science Report: SC020150/SR2, http://www.phillywatersheds.org/doc/ThamesEstuaryIodineSourceStudy.pdf, **2007**
29. **Reifenhäuser C. And Heumann K.,** *Development of a definitive method for iodine speciation in aquatic systems*, Fresenius' Journal of analytical Chemistry, Volume 336, Issue 7, Pages 559-563, **1990**.
30. **Rijn L.,** Tidal River Development: http://tide-project.eu/downloads/1203583-000-ZKS-0005-r-Comparison_Hydrodynamics_and_Salini-2.pdf, **2011**
31. **Semzhon T., et al.,** *Transport and distribution of artificial gamma-emitting radionuclides in the River Yenisei and its sediment*, Journal of Environmental Radioactivity, Volume 101, Issue 5, Pages 385-402, **2010**.
32**. Schnoor J.,** "Environmental Modeling: Fate and Transport of Pollutants in Water, Air and Soil", John Wiley and Sons, **1996.**
33. **Sundell-Bergman S., et al.,** *A new approach to assessment and management of the impact from medical liquid radioactive waste*, Journal of Environmental Radioactivity, Volume 99, Issue 10, Pages 1572-1577, **2008**.
34. **U.S. Environmental Protection Agency**: http://epa.gov/rpdweb00/radionuclides/iodine.html, **2012**
35. **Wikipedia**: http://en.wikipedia.org/wiki/Iodine-131, **2012**

Appendix

Appendix 1- Sediment data

The following tables provide sediment data obtained during the master work of former group students.

Table 1- Susanne Ulbrich's sediment data

Nr.	Date	Distance from WWTP [km]	Bank	Geographical Coordinates	Geometry	$C\left[\frac{Bq}{kg[DM]}\right]$
1	23.04.2008	17,5	left	N 53° 11' 44,9" E 8° 30' 59"	MB	<0,09
2	23.04.2008	12,75	left	N 53° 10' 25,8" E 8° 34' 23,58"	MB	0,65±0,08
3	23.04.2008	9,75	left	N 53° 9' 58,34" E 8° 37' 7,98"	MB	0,63±0,10
4	23.04.2008	5	left	N 53° 7' 21,47" E 8° 38' 56,51"	MB	0,46±0,19
5	23.04.2008	1,75	left	N 53° 7' 7,74" E 8° 41' 28,38"	MB	3,74±0,18
6	23.04.2008	0	left	N 53° 6' 58,6" E 8° 42' 56"	PD	98,71±2,28
7	04.05.2008	0	left	N 53° 6' 58,6" E 8° 42' 56"	PD	122,3±3,11
8	04.05.2008	2	left	N 53°6'32" E 8°44'20"	PD	2,51±0,87
9	04.05.2008	2,5	left	N 53°6'22" E 8°44'37"	PD	1,8±0,27
10	04.05.2008	4,5	left	N 53°5'30" E 8°45'45"	PD	2,34±0,38
11	04.05.2008	6,5	right	N 53°4'45" E 8°47'18"	MB	1,89±0,16
12	04.06.2008	20	right	N 53° 13' 03" E 8° 29' 55"	MB	0,45±0,045
13	04.06.2008	17,5	right	N 53° 11' 52" E 8° 31' 8"	MB	0,84±0,11
14	04.06.2008	14	right	N 53° 10' 53" E 8° 33' 44"	MB	0,75±0,07
15	04.06.2008	9,75	right	N 53° 10' 7" E 8° 37' 22"	MB	0,73±0,07
16	04.06.2008	4,5	right	N 53° 7'42" E 8° 39' 14"	PD	2,73±0,28
17	08.06.2008	0,5	right	N 53°7'11" E 8°42'48"	PD	1,75±0,47
18	08.06.2008	2,25	right	N 53°6'32"	PD	1,5±0,39

				E 8°44'44"		
19	08.06.2008	3,75	right	N 53°5'31,3" E 8°45'54,2"	PD	0
20	08.06.2008	6,5	right	N 53°4'52,4" E 8°47'21,4"	PD	1,6±0,26

Additional sediment data were collected from S.Ulbrich at 3.07.2012 in 4 locations in Weser river. Only the sediments in the WWTP outflow (0 km) gave activity above detection limit (26.9±1.0 and 26.9±1.4 Bk/kg[DM]), while in the other locations (6,12 and 18 km downstream) the activity was below detection limit.

Table 2- Philip Lysogne's sediment data

Sample ID	1	2	3	4
Collection date	23.06.2009	23.06.2009	23.06.2009	23.06.2009
Collection time	09:05	09:50	11:30	12:40
Latitude (N)	53°11'44''	53°07'21''	53°06'57''	53°06'30''
Longitude (E)	08°30'59''	08°38'55''	08°42'54''	08°44'18''
Geometry	1 L Marinelli	1 L Marinelli	1 L Marinelli	Petri dish
Wet mass(g)	1548.5	1252.3	1043.6	108.9
Dry mass(g)	634.3	329.3	98.6	56.3
Measurement date	23.06.2009	23.06.2009	23.06.2009	23.06.2009
C (Bk/kg[DM])	0,380 ±0,108	3,83±0,031	46,780±1,78	0,51±0,160

Sample ID	12	13	14	15
Collection date	04.07.2009	05.07.2009	05.07.2009	07.07.2009
Collection time	21:15	09:13	11:20	11:15
Latitude (N)	53°10'06''	53°10'41''	53°10'25''	53°06'51''
Longitude (E)	08°37'22''	08°33'47''	08°34'23''	08°43'23''
Geometry	1 L Marinelli	1 L Marinelli	Petri dish	1 L Marinelli
Wet mass(g)	1461.0	1448.2	77.5	1515.5
Dry mass(g)	560.5	561.1	33.1	399.5
Measurement date	04.07.2009	05.07.2009	05.07.2009	07.07.2009
C (Bk/kg[DM])	1.188±0.098	1.297±0.117	1.33±0.230	6.52±0.261

Sample ID	16	17	18	19
Collection date	07.07.2009	07.07.2009	07.07.2009	08.07.2009
Collection time	12:00	12:35	13:15	12:30
Latitude (N)	53°06'56''	53°07'03''	53°07'21''	53°03'41''
Longitude (E)	08°43'07''	08°42'34''	08°38'56''	08°51'39''
Geometry	Petri dish	Petri dish	Petri dish	1 L Marinelli
Wet mass(g)	87.1	87.6	70.2	1674.1
Dry mass(g)	23.2	19.8	20	683.0
Measurement date	07.07.2009	07.07.2009	07.07.2009	08.07.2009
C (Bk/kg[DM])	9.23±0.560	27.7±1.1	9.6±0.93	0.461±0.044

Sample ID	20	23	25
Collection date	08.07.2009	16.07.2009	20.07.2009
Collection time	13:05	15:40	09:25
Latitude (N)	53°03'45''	53°14'57''	53°03'49'
Longitude (E)	08°50'11''	08°28'21''	08°50'31''
Geometry	Petri dish	1 L Marinelli	1 L Marinelli
Wet mass(g)	72.2	1518.4	1774.7
Dry mass(g)	22.3	458.9	806.4
Measurement date	08.07.2009	18.07.2009	20.07.2009
C (Bk/kg[DM])	0.73±0.250	0.572±0.142	0.322±0.045

Appendix 2- Chemical yield determination data

The following tables provide a detailed description of the procedures and the results of the determination of the chemical yield for the two different methods described in Chapter 2.

Table 1: Chemical yield determination for "Method for determination of ^{131}I in surface water"

1.1 WWTP water: 23.01.2012/15:30

Sample	1	2	3	4
Description	Water (2Lt)	Filter 21mm (5Lt)	Filter 21mm (3 Lt)	Filter 21mm (3 Lt)
Mass (g)	1896.5	4318.0	2895.9	2743.9
Measured at	23.01.2012	27.01.2012	1.02.2012	3.02.2012
File	50607	30410	30413	30414
Measuring time(s)	324911	242954	149816	238613
Efficiency	eff51240	3_filter_21_nn_nn_nn	3_filter_21_nn_nn_nn	3_filter_21_nn_nn_nn
Activity concentration [mBq/kg]	110±1	20±2	30±4	10±2
Chemical yield	-	(18.2±2.5)%	(27.3±4.4)%	(35.4±5.2)%
Comment	Reference activity	Complete procedure	Complete procedure	2nd filtration chemical yield calculated as sum of activities samples 3 and 4

1.2 Iodine pills: 23.01.2012/15:30

Sample	1	2	3	4
Description	Gel	Filter 21mm (1Lt)	Filtered water (1Lt)	Precipitate (1 Lt)
Mass (g)	73.9	904.8	904.8	904.8
Measured at	14.02.2012	15.02.2012	15.02.2012	15.02.2012
File	60897	30422	60890	30423
Measuring time(s)	72723	7105	14854	81157
Efficiency	efk61470	3_filter_21_nn_nn_nn	efk61230	Det3_Petri(20mm)_Water_20_70_1-20
Activity concentration [mBq/kg]	6.5±0.3	5.5±0.4	1.6±0.1	0.35±0.1
Chemical yield	-	(84.3±6.7)%	-	(89.6±6.9)%
Comment	Reference activity	2nd filtration not complete procedure	2nd filtration not complete procedure	chemical yield calculated as sum of activities samples 2 and 4

1.3 Iodine pills: 13.05.2012/13:30

Sample	1	2	3
Description	Gel	Filter1 38mm (15Lt)	Filter2 38mm (15Lt)
Mass (kg)	0.074	15	15
Measured at	16.03.2012	16.03.2012	16.03.2012
File	60919	30444	30445
Measuring time(s)	7272	189	391
Efficiency	efk61470	3_filter_38_nn_nn_nn	3_filter_38_nn_nn_nn
Activity concentration [mBq/kg]	1057.8±17.3	424.3±23.0	305.1±16.5
Chemical yield	-	(70.8±2.9)%	-
Comment	Reference activity	not complete procedure chemical yield calculated as sum of activities samples 2,3 and 5	-

Sample	4	5
Description	Filtered water (15 Lt)	Precipitate (15 Lt)
Mass (kg)	1.0	15
Measured at	20.03.2012	16.03.2012

File	60925	60920
Measuring time(s)	81157	3523
Efficiency	efk61230	eff61470
Activity concentration [mBq/kg]	259.7±7.9	19.3±0.3
Chemical yield	-	-
Comment	-	-

1.4 WWTP water: 2.04.2012/10:45

Sample	1	2	3	4	5
Description	Water sample (1 Lt)	Water sample (1 Lt)	Filter 38mm (3Lt)	Filter 38mm (3Lt)	Filter 38mm (3 Lt)
Mass (g)	1047.3	999.8	3000.1	3007.5	3022.8
Measured at	2.04.2012	3.04.2012	3.04.2012	4.04.2012	5.04.2012
File	60934	50652	30460	30461	30464
Measuring time(s)	98965	85279	79086	80750	77885
Efficiency	efk61230	efk51230	3_filter_38_nn_nn_nn	3_filter_38_nn_nn_nn	3_filter_38_nn_nn_nn
Activity concentration [mBq/kg]	287±3	244±4	153±9	50±4	165±7
Chemical yield	-	-	(57.5±3.4)%	(20.7±1.5)%	(62.0±2.7)%
Comment	Mean value of samples 1 and 2 used as reference activity	not complete procedure	not complete procedure	not complete procedure	not complete procedure

1.5 WWTP water: 3.05.2012/10:00

Sample	1	2	3	4
Description	Water sample (1 Lt)	Filter 38mm (3Lt)	Filter 38mm (3Lt)	Filter 38mm (3Lt)
Mass (g)	986.4	3015.4	3015.4	1600.4
Measured at	3.05.2012	4.05.2012	4.05.2012	5.05.2012
File	50674	50675	60961	50676
Measuring time(s)	93999	89484	72407	15447
Efficiency	efk51230	-	-	-
Activity concentration	249±4	596±4	580±4	120±8

[mBq/kg]				
Chemical yield	-	(23.9±1.7)%	(23.3±1.7)%	(48.2±3.3)%
Comment	reference activity	not complete procedure	not complete procedure	not complete procedure

Sample	5	6
Description	Water sample (3 Lt)	Water sample (3 Lt)
Mass (g)	3011.3	3004.3
Measured at	18.04.2012	19.04.2012
File	30471	30472
Measuring time(s)	87784	84122
Efficiency	3_filter_38_nn_nn_nn	3_filter_38_nn_nn_nn
Activity concentration [mBq/kg]	278±5	355±1
Chemical yield	(10.5±1.8)%	(13.4±2.2)%
Comment	complete procedure	complete procedure

General comment: for samples 1.5, 2, 3 and 4 that efficiency is not stated, for all the filters the efficiency 3_filter_38_nn_nn_nn was used. No efficiency transfer was made and as a result errors of 10% range or more should be expected.

Table 2: Chemical yield determination for "Gamma spectrometric method for determination of radionuclides in surface water"

1.1 WWTP water: 21.05.2012/10:00 (original sampling was performed at 3.05.2012)

Sample	1	2	3	4	5
Description	Water (1Lt)	Precipitate (5Lt)	Precipitate (5 Lt)	Precipitate (5 Lt)	Precipitate (5 Lt)
Mass (g)	1010.6	4963.0	4961.5	4994.3	4992.1
Measured at	21.05.2012	22.05.2012	23.05.2012	24.05.2012	25.05.2012
File	50685	50686	50687	50688	50689
Measuring time(s)	94373	79428	81486	84408	83547
Efficiency	efk51230	efk51230	efk51230	efk51230	efk51230
Activity concentration [mBq/kg]	77.2±26.1	38.4±7.6	30.6±7.2	36.5±7.7	34.0±8.1
Chemical yield	-	(49.7±19.4)%	(39.6±16.3)%	(47.3±18.8)%	(44.0±18.2)%
Comment	Reference activity				

1.2 WWTP water: 31.05.2012/10:00 (original sampling was performed at 3.05.2012)

Sample	1	2	3	4	5
Description	Water (1Lt)	Water (2Lt)	Water (1 Lt)	Precipitate A (20 Lt)	Water after precipitate A
Mass (g)	1009.9	2003.2	1007.2	20010.3	2000.4
Measured at	31.05.2012	1.06.2012	4.06.2012	1.06.2012	2.06.2012
File	50690	50691	40391	60979	60980
Measuring time(s)	86230	238322	94287	75697	166873
Efficiency	efk51230	eff51240	efk41230	efk61230	efk61240-created
Activity concentration [mBq/kg]	171±29	95.3±16.8	145.1±43.4	95.5±3.3	54.7±13.8
Chemical yield	-	-	-	(63.6±4.7)%	-
Comment				Maximum value of chemical yield	

Sample	6	7	8	9	10
Description	Precipitate B (20 Lt)	Water after precipitation	Precipitate I (20 Lt)	Precipitate II (20 Lt)	Water sample V- top
Mass (g)	19921.5	1999.1	20007.9	20003.8	1998.7
Measured at	1.06.2012	2.06.2012	5.06.2012	5.06.2012	7.06.2012
File	40389	40390	40392	60986	50699
Measuring time(s)	76078	166655	75696	57573	86555
Efficiency	efk41230	efk41230	efk41230	efk61230	eff51240
Activity concentration [mBq/kg]	95.6±3.7	54.9±20.0	80.0±4.3	79.3±4.4	146.9±39.1
Chemical yield	(63.5±9.8) %	-	(58.4±13.8)%	(57.8±11.5)%	-
Comment	Maximum value of chemical yield		Reference activity: average of samples 1,2 and 3	Reference activity: average of samples 1,2 and 3	New containers used

Sample	11	12	13	14
Description	Water sample V-bottom	Precipitate V	Water sample III	Precipitate III (20 Lt)
Mass (g)	2186.7	19180.0	1992.9	19180.0
Measured at	7.06.2012	9.06.2012	7.06.2012	9.06.2012
File	30514	50703	40394	40395

Measuring time(s)	78840	81147	162822	81764
Efficiency	3_mar2-2_190_93_1-0_water	efk51230	efk41240-created	efk41230
Activity concentration [mBq/kg]	172.3±24.8	97.9±5.0	128.6±34.9	79.9±4.8
Chemical yield	-	(61.3±9.4)%	-	(62.1±17.3)%
Comment		New containers used- Reference activity: average of samples 10 and 11.		New containers used- Reference activity: sample 13

Sample	15	16
Description	Water sample IV	Precipitate IV
Mass (g)	2003.0	18780.0
Measured at	7.06.2012	9.06.2012
File	60989	60991
Measuring time(s)	163639	80771
Efficiency	efk61240-created	efk61230
Activity concentration [mBq/kg]	105.0±23.0	69.6±4.5
Chemical yield	-	(66.3±15.1)%
Comment		New containers used- Reference activity: sample 15

Appendix 3- Sampling data

The following tables provide a detailed description of the sampling locations and results of this study as explained in Chapter 3.

Table 1: Sampling campaign #1

Sample	1	2	3
Latitude N	53.05942	53.0746848	530.800.513
Longitude E	8.5262	8.8033550	87.916.655
date of sampling	21.06.2012	21.06.2012	21/6/2012
time of sampling	6:50	8:29	8:37
tide during sampling	HT->LT	HT->LT	HT->LT
Mass (kg)	20.08	20.32	20.22
measured at	22.06.2012	22.06.2012	23.06.2012
file	30541	40404	61020
measuring time (s)	87589	86570	91440
efficiency	3_mar1-0_14l_100_1_00_water	efk41230	efk61230
Activity concentration[mBq/kg]	< 2.6	< 3.9	< 3.4

Sample	4	5	6	7
latitude	53.0943026	53.1176365	53.1189690	53.1237193
longitude	8.7613274	8.7217211	8.7004711	8.6773089
date of sampling	21.06.2012	21.06.2012	21.062012	21.06.2012
time of sampling	8:46	9:01	9:05	9:09
tide during sampling	HT->LT	HT->LT	HT->LT	HT->LT
Mass (kg)	17.64	19.78	18.16	20.30
measured at	23.06.2012	24.06.2012	27.06.2012	27.06.2012
File	40405	40406	50738	61026
measuring time (s)	91539	84889	83815	83777
efficiency	efk41230	efk41230	efk51230	efk61230
Activity concentration[mBq/kg]	< 4.6	< 4.7	< 6.5	< 5.1

Sample	8	9	10
latitude	53.1274369	53.1399654	53.1563479
longitude	8.6512045	8.6318358	8.6271664
date of sampling	21.06.2012	21.06.2012	21.06.2012
time of sampling	9:19	9:24	9:28
tide during sampling	HT->LT	HT->LT	HT->LT
Mass (kg)	18.80	18.74	19.76
measured at	26.6.2012	26.6.2012	24.06.2012
File	50737	61025	61021
measuring time (s)	88040	87360	84196
efficiency	efk51230	efk61230	efk61230
Activity	< 5.5	< 4.9	< 4.0

concentration[mBq/kg]			

Table 2: Sampling campaign #2

Sample	11	12
latitude	53.11641	53.11635
longitude	8.71525	8.71559
date of sampling	3.07.2012	3.07.2012
time of sampling	13:10	13:25
tide during sampling	LT->HT	LT->HT
Mass (kg)	20.14	20.30
measured at	5.07.2012	5.07.2012
File	30557	61034
measuring time (s)	74213	78029
efficiency	3_mar1-0_14l_100_1_00_water	efk61230
Activity concentration[mBq/kg]	9.6±1.4	9.5±1.3

Table 3: Sampling campaign #3

Sample	13	14	15	16
latitude	53.116086	53.1145	53.111506	53.108.719
longitude	8.717206	8.722436	8.727997	8.731.219
date of sampling	5.07.2012	5.07.2012	5.07.2012	5/7/2012
time of sampling	13:27	13:41	13:52	14:04
tide during sampling	LT->HT	LT->HT	LT->HT	LT->HT
Mass (kg)	20.04	20.08	20.40	20.04
measured at	6.07.2012	6.07.2012	7.07.2012	7.07.2012
File	30558	61035	61036	50749
measuring time (s)	84366	84521	82631	82824
efficiency	3_mar1-0_14l_100_1_00_water	efk61230	efk61230	efk51230
Activity concentration[mBq/kg]	21.9±1.8	< 3.4	< 3.7	< 4.2

Table 4: Sampling campaign #4

Sample	17	18	19	20
latitude	53.116572	53.117481	53.117533	53.117567
longitude	8.7148	8.707653	8.701722	8.695825
date of sampling	9.07.2012	9.07.2012	9.07.2012	9.07.2012
time of sampling	9:56	10:06	10:15	10:25

tide during sampling	HT->LT	HT->LT	HT->LT	HT->LT
Mass (kg)	20.32	20.04	20.74	20.04
measured at	11.07.2012	11.07.2012	10.07.2012	10.07.2012
File	50751	40422	50750	40421
measuring time (s)	76852	764211	80573	80438
efficiency	efk51230	efk41230	efk51230	efk41230
Activity concentration[mBq/kg]	50.3±7.6	7.9±2.5	5.7±2.6	< 4.1

Table 5: WWTP effluent measurements

Corresponding sampling campaign	2	3	4
date of sampling	3.07.2012	5.07.2012	9.07.2012
time of sampling	13:50	13:04	9:40
Mass (kg)	4.00	3.96	3.88
measured at	3.07.2012	7.07.2012	10.07.2012
File	30553	30559	30560
measuring time (s)	65532	83056	81703
efficiency	3_mar2-4_190_163_1-0_water_nc	3_mar2-4_190_163_1-0_water_nc	3_mar2-4_190_163_1-0_water_nc
Activity concentration[mBq/kg]	121.1±12.3	219.5±18.0	239.0±16.0

Appendix 4- IMIS data

In the following table, measurement results for ^{131}I for sewage effluent in the location of Bremen for the period 2000-2012 are given. (Source: IMIS- "Integrated Measuring and Information System for the Surveillance of Environmental Radioactivity")

Sampling date	Units	Measurement (I 131)	Measurement error (I 131) (%)
7/1/2000	Bq/l	4,11E-02	20,8
6/4/2000	Bq/l	8,64E-02	13,4
7/12/2000	Bq/l	1,64E-01	6,3
16/2/2001	Bq/l	2,47E-01	4,7
19/4/2001	Bq/l	< 3,00E-02	Null
6/9/2001	Bq/l	9,89E-02	28,9
12/10/2001	Bq/l	< 3,61E-02	Null
6/2/2002	Bq/l	1,59E-01	11
8/5/2002	Bq/l	9,87E-02	9,8

10/9/2002	Bq/l	1,30E-01	10,8
8/11/2002	Bq/l	1,42E-01	11,1
5/3/2003	Bq/l	1,61E-01	10,1
18/6/2003	Bq/l	1,61E-01	15,4
8/9/2003	Bq/l	6,03E-02	29,8
16/10/2003	Bq/l	1,29E-01	12
28/1/2004	Bq/l	4,66E-01	4,4
9/6/2004	Bq/l	1,92E-01	13,2
22/7/2004	Bq/l	1,14E-01	14,2
4/11/2004	Bq/l	1,84E-01	9,2
16/2/2005	Bq/l	4,95E-01	5,5
26/5/2005	Bq/l	1,03E-01	13,4
23/8/2005	Bq/l	2,37E-01	12,7
8/12/2005	Bq/l	2,46E-01	9,3
25/1/2006	Bq/l	2,94E-01	13,1
31/5/2006	Bq/l	1,28E-01	21,8
1/9/2006	Bq/l	1,37E-01	23,2
12/12/2006	Bq/l	3,19E-01	14,6
8/2/2007	Bq/l	9,77E-01	4,8
20/4/2007	Bq/l	3,24E-01	7,4
21/9/2007	Bq/l	2,20E-01	18,3
11/12/2007	Bq/l	3,00E-01	10,4
23/1/2008	Bq/l	2,25E-01	16,5
24/4/2008	Bq/l	3,99E-01	7,3
10/7/2008	Bq/l	< 1,01E-01	Null
3/12/2008	Bq/l	4,55E-01	8,1
10/2/2009	Bq/l	2,79E-01	10,7
16/4/2009	Bq/l	1,56E-01	17,5
24/9/2009	Bq/l	2,35E-01	13
28/10/2009	Bq/l	2,54E-01	14,1
13/1/2010	Bq/l	2,53E-01	15,4
4/5/2010	Bq/l	2,12E-01	14,6
16/8/2010	Bq/l	1,40E-01	23
17/12/2010	Bq/l	2,59E-01	8,2
23/2/2011	Bq/l	2,68E-01	11,9
23/6/2011	Bq/l	2,33E-01	13,1
7/9/2011	Bq/l	2,39E-01	13
8/11/2011	Bq/l	3,12E-01	10,4
3/2/2012	Bq/l	1,85E-01	4,8
11/5/2012	Bq/l	2,52E-01	16,9
10/2/2012	Bq/l	<7,98E-02	Null

Appendix 5- WWTP outflow data

In the following tables the discharge values from the WWTP during the dates of sampling are given.

Table 1: Discharge from WWTP during the 1st and 2nd sampling campaigns

Date and time	Discharge (m^3/s)	Date and time	Discharge (m^3/s)
21/6/2012 00:00:00	1,10	3/7/2012 00:00:00	1,10
21/6/2012 01:00:00	1,14	3/7/2012 01:00:00	1,16
21/6/2012 02:00:00	1,02	3/7/2012 02:00:00	1,14
21/6/2012 03:00:00	0,88	3/7/2012 03:00:00	1,07
21/6/2012 04:00:00	0,92	3/7/2012 04:00:00	1,04
21/6/2012 05:00:00	1,01	3/7/2012 05:00:00	0,96
21/6/2012 06:00:00	0,89	3/7/2012 06:00:00	0,89
21/6/2012 07:00:00	0,86	3/7/2012 07:00:00	0,89
21/6/2012 08:00:00	0,95	3/7/2012 08:00:00	1,03
21/6/2012 09:00:00	1,10	3/7/2012 09:00:00	1,00
21/6/2012 10:00:00	1,18	3/7/2012 10:00:00	1,10
21/6/2012 11:00:00	1,17	3/7/2012 11:00:00	1,30
21/6/2012 12:00:00	1,27	3/7/2012 12:00:00	1,36
21/6/2012 13:00:00	1,32	3/7/2012 13:00:00	1,35
21/6/2012 14:00:00	1,22	3/7/2012 14:00:00	1,30
21/6/2012 15:00:00	1,21	3/7/2012 15:00:00	0,96
21/6/2012 16:00:00	1,30	3/7/2012 16:00:00	0,93
21/6/2012 17:00:00	1,34	3/7/2012 17:00:00	0,82
21/6/2012 18:00:00	1,27	3/7/2012 18:00:00	0,92
21/6/2012 19:00:00	1,20	3/7/2012 19:00:00	0,99
21/6/2012 20:00:00	1,14	3/7/2012 20:00:00	0,97
21/6/2012 21:00:00	1,04	3/7/2012 21:00:00	0,99
21/6/2012 22:00:00	1,07	3/7/2012 22:00:00	1,40
21/6/2012 23:00:00	1,16	3/7/2012 23:00:00	1,41
22/6/2012 00:00:00	1,11	4/7/2012 00:00:00	1,02

Table 2: Discharge from WWTP during the 3rd and 4th sampling campaigns

Date and time	Discharge (m^3/s)	Date and time	Discharge (m^3/s)
5/7/2012 00:00:00	1,21	9/7/2012 00:00:00	2,04
5/7/2012 01:00:00	1,27	9/7/2012 01:00:00	2,07
5/7/2012 02:00:00	1,39	9/7/2012 02:00:00	1,97
5/7/2012 03:00:00	1,32	9/7/2012 03:00:00	1,80
5/7/2012 04:00:00	1,13	9/7/2012 04:00:00	1,52
5/7/2012 05:00:00	1,02	9/7/2012 05:00:00	1,06
5/7/2012 06:00:00	1,03	9/7/2012 06:00:00	0,91
5/7/2012 07:00:00	1,19	9/7/2012 07:00:00	0,89
5/7/2012 08:00:00	1,27	9/7/2012 08:00:00	1,01
5/7/2012 09:00:00	1,28	9/7/2012 09:00:00	1,20
5/7/2012 10:00:00	1,28	9/7/2012 10:00:00	1,35
5/7/2012 11:00:00	1,26	9/7/2012 11:00:00	1,32

5/7/2012 12:00:00	1,29	9/7/2012 12:00:00	1,22
5/7/2012 13:00:00	1,15	9/7/2012 13:00:00	1,25
5/7/2012 14:00:00	1,13	9/7/2012 14:00:00	1,11
5/7/2012 15:00:00	1,15	9/7/2012 15:00:00	1,10
5/7/2012 16:00:00	1,18	9/7/2012 16:00:00	1,35
5/7/2012 17:00:00	1,11	9/7/2012 17:00:00	2,02
5/7/2012 18:00:00	1,06	9/7/2012 18:00:00	2,41
5/7/2012 19:00:00	1,12	9/7/2012 19:00:00	2,53
5/7/2012 20:00:00	1,12	9/7/2012 20:00:00	2,76
5/7/2012 21:00:00	1,11	9/7/2012 21:00:00	2,69
5/7/2012 22:00:00	1,17	9/7/2012 22:00:00	2,56
5/7/2012 23:00:00	1,08	9/7/2012 23:00:00	2,29
6/7/2012 00:00:00	1,05	10/7/2012 00:00:00	1,98

Appendix 6- Weser hydrological data

The hydrological data from different stations along the Weser River and a calendar with tide predictions are given in the next tables.

Hydrologische Werte der Weser und Nebenflüsse **PN**

	Pegel	Pegel-Null	Gruppe	Standort	MThw 1996/05	MTnw 1996/05	MThb 1996/05	SKN [LAT]	HHThw		NNTnw		mitt. Flut- u. Ebbedauer T_z	T_u	mitt. Flut u. Ebbestromdauer T_f	T_e	Kenterung am Pegel t_k	t_{k_e}	Stromgeschwindigkeit Mittel V_m	V_{em}	Max V_{max}	V_{emax}	Eintrittszeitdifferenzen bezogen auf Pegel Bremerhaven Thw	Tnw	k_f	k_{f_e}
		NN - m		km	PN+cm	PN+cm	PN+cm	PN+cm	PN+cm	Datum	PN+cm	Datum	h.min	h.min	h.min	h.min	h.min	h.min	cm/s	cm/s	cm/s	cm/s	h.min	h.min	h.min	h.min
Weser	Weserwehr UW	5,01	b	362,780re	759	361	398	301	1126	6.1.26	191	25.1.96	05:00	07:25	—	12:25	—	—	—	30	—	60	01:48	03:00	—	—
	Gr. Weserbrücke	5,00	a	0,030 li	752	342	410	300	1043	28.1.94	188	25.1.96	05:08	07:18	00:30	11:55	-3:55	00:25	5	30	15	65	01:47	02:51	-02:09	03:16
	Oslebshausen	5,01	a	8,375 re	748	336	412	301	1035	17.12.62	178	15.3.64	05:20	07:06	05:07	07:12	00:18	00:19	30	45	50	65	01:39	02:32	01:56	02:49
	Vegesack	5,00	a	17,850 re	736	345	391	300	1033	28.1.94	171	15.3.64	05:31	06:54	05:00	07:20	00:14	00:33	40	50	100	80	01:30	02:11	01:44	02:43
	Farge	5,01	b	26,260 re	724	342	382	301	1030	3.1.76	158	15.3.64	05:40	06:45	04:55	07:30	00:25	00:40	75	80	120	100	01:15	01:48	01:40	02:27
	Elsfleth	5,06	b	33,330 li	724	338	386	293	1025	17.2.62	145	15.3.64	05:48	06:38	05:25	07:00	00:30	00:50	70	80	110	100	01:01	01:25	01:32	02:17
	Brake	5,00	a	39,195 li	709	319	390	275	1029	17.2.62	125	15.3.64	05:54	06:32	05:30	06:55	00:35	00:56	65	80	90	100	00:48	01:07	01:23	02:03
	Nordenham	4,98	b	55,800 li	693	298	395	238	1019	16.2.62	98	15.3.64	06:12	06:13	06:15	06:15	00:47	00:51	81	92	121	131	00:21	00:21	01:08	01:12
	Bremerhaven	4,98	a	66,670 re	679	303	376	243	1035	16.2.62	81	15.3.64	06:12	06:32	06:00	06:30	00:50	01:03	84	104	146	159	—	—	00:50	01:03
	Alte Weser	4,96	a	115,00	633	346	287	281	904	3.1.76	160	17.3.69	05:53	06:32	06:22	06:00	01:08	00:28	63	53	111	114	-01:20	-01:02	-00:15	-00:38
								KN																		
Jade	Oldenb. - Drielake	5,01	a	0,528 li	721	460	261	421	843	17.2.62	306	8.12.59	05:01	07:25	04:50	07:35	00:00	00:10	20	25	30	35	02:25	03:36	02:25	03:45
	Reithörne	5,01	b	7,550 li	712	459	253	421	846	17.2.62	305	8.12.59	05:20	07:05	05:05	07:20	00:16	00:30	45	50	60	65	02:13	03:06	02:30	03:24
	Hollersiel	4,99	b	11,535 re	705	435	270	419	927	3.1.76	277	8.12.59	05:36	06:59	05:15	07:05	00:30	00:50	60	65	70	75	01:55	02:43	02:27	03:33
	Buttelerhörne	5,00	b	14,247 re	707	419	288	388	965	3.1.76	259	8.12.59	05:28	06:58	05:20	07:05	00:35	00:45	55	60	75	85	01:41	02:27	02:18	03:12
	Huntebrück	5,00	b	17,810 li	714	365	349	336	1008	3.1.76	235	8.12.59	05:32	06:53	05:35	06:45	00:45	00:40	65	85	95	110	01:18	01:59	02:05	02:40
	Elsfleth / Ohrt	5,00	b	20,780 re	719	339	380	294	1025	3.1.76	166	15.3.64	05:40	06:46	05:35	06:45	00:30	00:35	40	45	60	65	01:09	01:41	01:40	02:17
Hamme Lesum	Wasserhorst	4,99	b	2,255 li	725	423	302	—	967	3.1.76	292	25.1.96	04:59	07:22	04:51	07:32	00:40	00:50	60	65	80	80	01:56	03:07	02:37	03:57
	Ritterhude	5,01	b	1,860 re	723	441	282	—	927	3.1.76	312	15.3.64	04:39	07:42	—	12:25	—	—	—	20	—	40	02:02	03:32	—	—
	Niederblockland	5,01	b	8,000 li	700	498	202	—	880	17.2.62	396	21.10.99	04:37	07:49	04:15	08:10	00:20	00:20	45	40	65	60	03:01	04:46	03:22	05:07
Wümme	Borgfeld	5,01	b	0,265 re	694	589	105	—	852	17.2.62	468	22.8.76	04:13	08:12	01:53	10:29	00:10	01:50	6	15	10	40	04:12	06:12	04:11	07:58

$MQ_{Intschede\ 40/05}$ = 325 m³/s	$MQ_{U\text{-}Hunte\ 40/05}$ = 14,6 m³/s	$MQ_{Hellwege\ 05/05}$ = 9,24 m³/s

Die statistischen Werte der Nebenflüsse wurden aus den unbeeinflußten Werten ermittelt.

$BHHThw_{Hunte}$ PN = 830 cm ; $BHHThw_{Lesum,\ Wümme,\ Hamme}$ PN = 820 cm (PN = NN -5,00 m)

Lesum km 0,00 = Wümme km 18,52

HHThw + NNTnw bezogen auf das zum Eintrittszeitpunkt gültige PN

Lesum - Mündung km 9,85 bei UWe km 17,49

UWe km 0,0 = MWe km 366,725

Hunte - Mündung km 24,63 bei UWe km 32,09

Achse Weserwehr Mwe km 362,153

Wasser- und Schifffahrtsamt Bremen
Gewässerkunde

Aufgestellt	Bearbeitet: Schmele	
Dipl.-Ing. Piechotta	Mastrangelo	Stand 15.01.08

Figure I: Hydrological data for Weser River from different stations

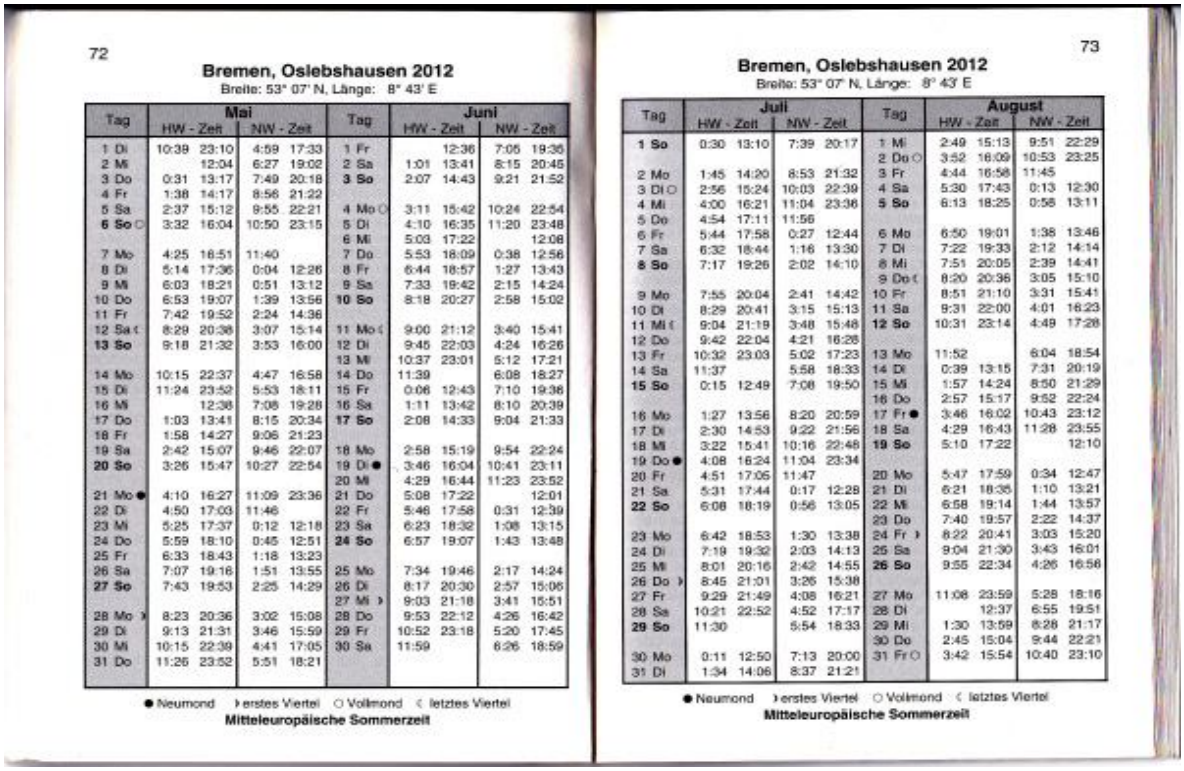

72

Bremen, Oslebshausen 2012

Breite: 53° 07' N, Länge: 8° 43' E

Tag	Mai HW - Zeit	Mai NW - Zeit			Tag	Juni HW - Zeit	Juni NW - Zeit	
1 Di	10:39	23:10	4:59	17:33	1 Fr		12:36	7:05 19:36
2 Mi		12:04	6:27	19:02	2 Sa	1:01	13:41	8:15 20:45
3 Do	0:31	13:17	7:49	20:18	**3 So**	2:07	14:43	9:21 21:52
4 Fr	1:38	14:17	8:56	21:22				
5 Sa	2:37	15:12	9:55	22:21	4 Mo ○	3:11	15:42	10:24 22:54
6 So ○	3:32	16:04	10:50	23:15	5 Di	4:10	16:35	11:20 23:48
					6 Mi	5:03	17:22	12:08
7 Mo	4:25	16:51	11:40		7 Do	5:53	18:09	0:38 12:56
8 Di	5:14	17:36	0:04	12:26	8 Fr	6:44	18:57	1:27 13:43
9 Mi	6:03	18:21	0:51	13:12	9 Sa	7:33	19:42	2:15 14:24
10 Do	6:53	19:07	1:39	13:56	**10 So**	8:18	20:27	2:58 15:02
11 Fr	7:42	19:52	2:24	14:36				
12 Sa ☾	8:29	20:38	3:07	15:14	11 Mo ☾	9:00	21:12	3:40 15:41
13 So	9:18	21:32	3:53	16:00	12 Di	9:45	22:03	4:24 16:26
					13 Mi	10:37	23:01	5:12 17:21
14 Mo	10:15	22:37	4:47	16:58	14 Do	11:39		6:08 18:27
15 Di	11:24	23:52	5:53	18:11	15 Fr	0:06	12:43	7:10 19:36
16 Mi		12:38	7:08	19:28	16 Sa	1:11	13:42	8:10 20:39
17 Do	1:03	13:41	8:15	20:34	**17 So**	2:08	14:33	9:04 21:33
18 Fr	1:58	14:27	9:06	21:23				
19 Sa	2:42	15:07	9:46	22:07	18 Mo	2:58	15:19	9:54 22:24
20 So	3:26	15:47	10:27	22:54	19 Di ●	3:46	16:04	10:41 23:11
					20 Mi	4:29	16:44	11:23 23:52
21 Mo ●	4:10	16:27	11:09	23:36	21 Do	5:08	17:22	12:01
22 Di	4:50	17:09	11:46		22 Fr	5:46	17:58	0:31 12:39
23 Mi	5:25	17:37	0:12	12:18	23 Sa	6:23	18:32	1:08 13:15
24 Do	5:59	18:10	0:45	12:51	**24 So**	6:57	19:07	1:43 13:48
25 Fr	6:33	18:43	1:18	13:23				
26 Sa	7:07	19:16	1:51	13:55	25 Mo	7:34	19:46	2:17 14:24
27 So	7:43	19:53	2:25	14:29	26 Di	8:17	20:30	2:57 15:06
					27 Mi ☽	9:03	21:18	3:41 15:51
28 Mo ☽	8:23	20:36	3:02	15:08	28 Do	9:53	22:12	4:26 16:42
29 Di	9:13	21:31	3:46	15:59	29 Fr	10:52	23:18	5:20 17:45
30 Mi	10:15	22:39	4:41	17:05	30 Sa	11:59		6:26 18:59
31 Do	11:26	23:52	5:51	18:21				

● Neumond ☽ erstes Viertel ○ Vollmond ☾ letztes Viertel

Mitteleuropäische Sommerzeit

73

Bremen, Oslebshausen 2012

Breite: 53° 07' N, Länge: 8° 43' E

Tag	Juli HW - Zeit	Juli NW - Zeit			Tag	August HW - Zeit	August NW - Zeit	
1 So	0:30	13:10	7:39	20:17	1 Mi	2:49	15:13	9:51 22:29
					2 Do ○	3:52	16:09	10:53 23:25
2 Mo	1:45	14:20	8:53	21:32	3 Fr	4:44	16:58	11:45
3 Di ○	2:56	15:24	10:03	22:39	4 Sa	5:30	17:43	0:13 12:30
4 Mi	4:00	16:21	11:04	23:36	**5 So**	6:13	18:25	0:58 13:11
5 Do	4:54	17:11	11:56					
6 Fr	5:44	17:58	0:27	12:44	6 Mo	6:50	19:01	1:38 13:46
7 Sa	6:32	18:44	1:16	13:30	7 Di	7:22	19:33	2:12 14:14
8 So	7:17	19:26	2:02	14:10	8 Mi	7:51	20:05	2:39 14:41
					9 Do ☾	8:20	20:36	3:05 15:10
9 Mo	7:55	20:04	2:41	14:42	10 Fr	8:51	21:10	3:31 15:41
10 Di	8:29	20:41	3:15	15:13	11 Sa	9:31	22:00	4:01 16:23
11 Mi ☾	9:04	21:19	3:48	15:48	**12 So**	10:31	23:14	4:49 17:28
12 Do	9:42	22:04	4:21	16:26				
13 Fr	10:32	23:03	5:02	17:23	13 Mo	11:52		6:04 18:54
14 Sa	11:37		5:58	18:33	14 Di	0:39	13:15	7:31 20:19
15 So	0:15	12:49	7:08	19:50	15 Mi	1:57	14:24	8:50 21:29
					16 Do	2:57	15:17	9:52 22:24
16 Mo	1:27	13:56	8:20	20:59	17 Fr ●	3:46	16:02	10:43 23:12
17 Di	2:30	14:53	9:22	21:56	18 Sa	4:29	16:43	11:28 23:55
18 Mi	3:22	15:41	10:16	22:48	**19 So**	5:10	17:22	12:10
19 Do ●	4:08	16:24	11:04	23:34				
20 Fr	4:51	17:05	11:47		20 Mo	5:47	17:59	0:34 12:47
21 Sa	5:31	17:44	0:17	12:28	21 Di	6:21	18:35	1:10 13:21
22 So	6:08	18:19	0:56	13:05	22 Mi	6:58	19:14	1:44 13:57
					23 Do	7:40	19:57	2:22 14:37
23 Mo	6:42	18:53	1:30	13:38	24 Fr ☽	8:22	20:41	3:03 15:20
24 Di	7:19	19:32	2:03	14:13	25 Sa	9:04	21:30	3:43 16:01
25 Mi	8:01	20:16	2:42	14:55	**26 So**	9:55	22:34	4:26 16:56
26 Do ☽	8:45	21:01	3:25	15:38				
27 Fr	9:29	21:49	4:08	16:21	27 Mo	11:08	23:59	5:28 18:16
28 Sa	10:21	22:52	4:52	17:17	28 Di		12:37	6:55 19:51
29 So	11:30		5:54	18:33	29 Mi	1:30	13:59	8:28 21:17
					30 Do	2:45	15:04	9:44 22:21
30 Mo	0:11	12:50	7:13	20:00	31 Fr ○	3:42	15:54	10:40 23:10
31 Di	1:34	14:06	8:37	21:21				

● Neumond ☽ erstes Viertel ○ Vollmond ☾ letztes Viertel

Mitteleuropäische Sommerzeit

Figure II: Tide predictions for the months May- August 2012

Appendix 7- Additional spectra

In this appendix additional spectra are given from material used to create the final measured sample and could have possible contributed to an increase of the ^{131}I activity. As we observe they don't, however some of the other isotopes found in our samples could have originated from these material.

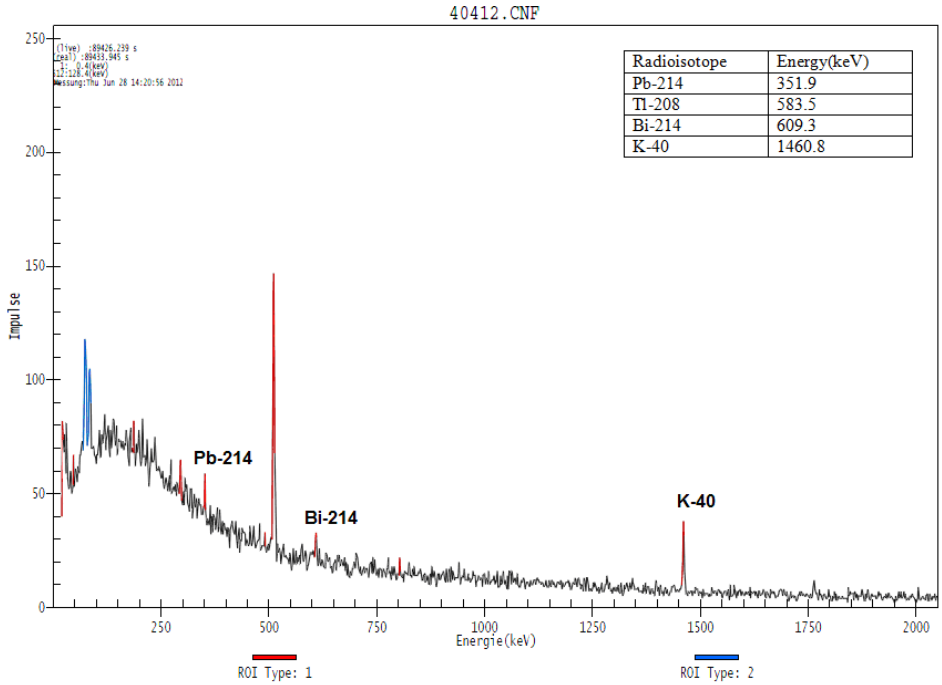

Radioisotope	Energy(keV)
Pb-214	351.9
Tl-208	583.5
Bi-214	609.3
K-40	1460.8

Figure III: Spectrum from a glue sample (m=52.6g, t_m=89426s, efk41470)

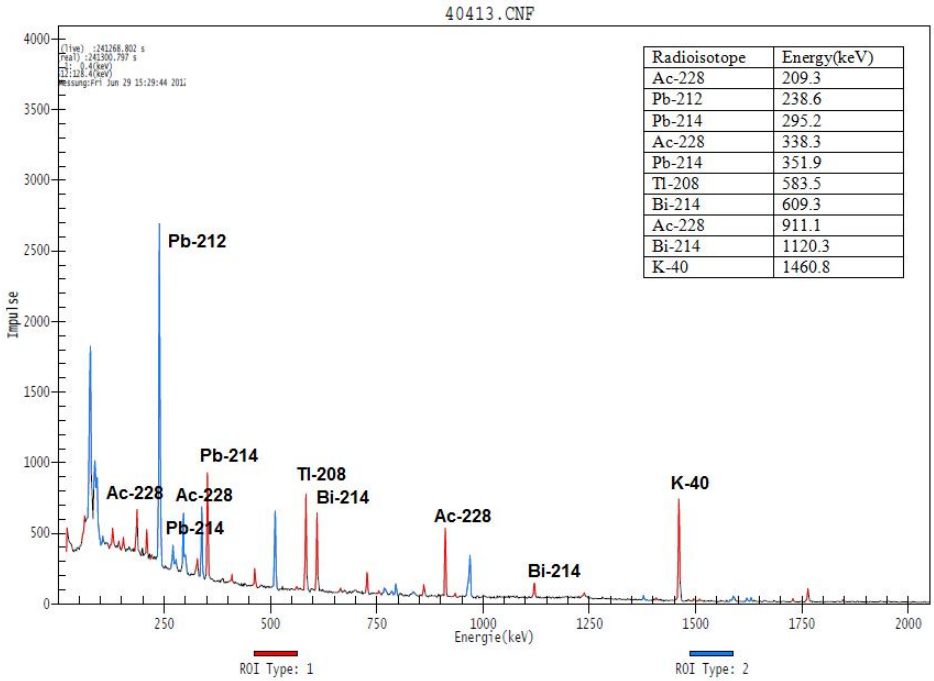

Radioisotope	Energy(keV)
Ac-228	209.3
Pb-212	238.6
Pb-214	295.2
Ac-228	338.3
Pb-214	351.9
Tl-208	583.5
Bi-214	609.3
Ac-228	911.1
Bi-214	1120.3
K-40	1460.8

Figure IV: Spectrum from a bentonite sample (m=65.4g, t_m=241268s, efk41470)

Appendix 8- Error propagation

This table shows the variances of simple functions of the real uncorrelated variable A, B with standard deviations σ_A and σ_B and precisely known real-valued constants a, b.

Function	Variance
$f = a \cdot A$	$\sigma_f = \sqrt{a^2 \cdot \sigma_A^2}$
$f = a \cdot A \pm b \cdot B$	$\sigma_f = \sqrt{a^2 \cdot \sigma_A^2 + b^2 \cdot \sigma_B^2}$
$f = A \cdot B$ or $f = \frac{A}{B}$	$\sigma_f = f\sqrt{\left(\frac{\sigma_A}{A}\right)^2 + \left(\frac{\sigma_B}{B}\right)^2}$
$f = a \cdot A^{\pm b}$	$\sigma_f = f \cdot b \cdot \frac{\sigma_A}{A}$
$f = a \cdot \ln(\pm b \cdot A)$	$\sigma_f = a \cdot \frac{\sigma_A}{A}$
$f = a \cdot \log(A)$	$\sigma_f = a \cdot \frac{\sigma_A}{A \cdot \ln(10)}$
$f = a \cdot e^{\pm b \cdot A}$	$\sigma_f = f \cdot b \cdot \sigma_A$
$f = a^{\pm b \cdot A}$	$\sigma_f = f \cdot b \cdot \ln(a) \cdot \sigma_A$

Appendix 9- Matlab script

In this appendix the m-files for the simulation of the activity concentration of ^{131}I in water and in sediment are given.

1. M-file activity concentration in water

```
%%water%%

%experimental data 2012
yy=[-112.2,0,126.5,503.5,996.6];
CC=[21.85,95.8,50.3,7.89,5.66];
errorCC=[1.82,9.5,7.56,2.53,2.55];

%setting of parameters
M=121*0.8;
D=0.48;  % D=0.1
kl=10^(-5);
d=1.5*10^(-3);
kpw=10;
Sw=10^(-5);
k=kl/(d*(1+kpw*Sw));
u=0.30;

l1=(u+sqrt((u^2)+4*D*k))/2*D;
l2=(u-sqrt((u^2)+4*D*k))/2*D;
```

```
% creation of arrays
x=[];
C=[];
Cj=[];
Ci=[];
xj=[];
xi=[];
xj(1)=1;
xi(1)=1;

    for j=1:500
        y=1;
        Cj(j)=M*exp(l1*(-j))*exp(l1*(y));
        xj(j)=j;
    end

   for k=1:500
       xj(k)=xj(k)*(-1);
   end

   xj=fliplr(xj);
   Cj=fliplr(Cj);

 for i=1:2000
     y=1;

        Ci(i)=M*exp(l2*i)*exp(-l2*(y));

       xi(i)=i;

 end
    for z=1:499
        C(z)=Cj(z);

        x(z)=xj(z);
    end
    C(500)=M;
    for z=501:2000
        C(z)=Ci(z-500);

        x(z)=xi(z-500);
    end

figure
plot (x,C)
title('Radionuclide concentration in water in the river');
xlabel('Distance from WWTP(m)');
ylabel('I-131 concentration in water(mBq/l)')
hold all;
errorbar(yy,CC,errorCC,'rd');
legend ('Model simulation','Experimental data');
```

2. M-file activity concentration in sediment

```
%%sediment**

%experimental data 2008-2009
```

```
xx=[-1500,-550,0,1500,3000,5000];
rr=[6.52,9.23,89.26,27.7,9.6,2.145];
errorrr=[0.261,0.56,2.28,3.11,1.78,1.1];


%setting of parameters
M=121*0.8;
D=0.48;
ks=10^(-4);
u=0.3;
L=5.3;
l=10^(-6);
d=1.5*10^(-3);
g=L/d;
Sw=10^(-5);
Sb=2.650;
kpb=10^4;
kpw=10;
a=2.5*10^(-6);
kl=10^(-5);
d=1.5*10^(-3);
kpw=10;
Sw=10^(-5);
k=kl/(d*(1+kpw*Sw));

l1=(u+sqrt((u^2)+4*D*k))/2*D;
l2=(u-sqrt((u^2)+4*D*k))/2*D;

alpha= ks*kpw*Sw*g/(Sb+(1/kpb));
beta=kl/(d*(Sb+(1/kpb))*(1+kpw*Sw));
gamma=l/(1+kpb*Sb);
delta=a*Sb/(Sb+(1/kpb));
epsilon=kl/(d*kpb*(Sb+(1/kpb)));

% creation of arrays
x=[];
C=[];
r=[];
Cj=[];
Ci=[];
xj=[];
xi=[];
Cr=[];
Crj=[];
Cri=[];
xj(1)=1;
xi(1)=1;
 factor=((alpha+beta)/(gamma+delta+epsilon));


    for j=1:1000
         Cj(j)=M*exp(l1*(-j));
         rj(j)=factor*Cj(j)/1000; %the division by 1000 is done to
convert the mBq into Bq
         xj(j)=j;
    end
   for k=1:1000
       xj(k)=xj(k)*(-1);
   end
```

```
   xj=fliplr(xj);
   Cj=fliplr(Cj);
   rj=fliplr(rj);

    for i=1:6000
        Ci(i)=M*exp(l2*i);
        ri(i)=factor*Ci(i)/1000; %the division by 1000 is done to
convert the mBq into Bq
        xi(i)=i;
    end
    for z=1:1000
        C(z)=Cj(z);
        x(z)=xj(z);
          r(z)=rj(z);
    end
    for z=1001:6000
        C(z)=Ci(z-1000);
        x(z)=xi(z-1000);
       r(z)=ri(z-1000);
    end

figure
plot (x,r,'k')
title('Radionuclide concentration in bottom sediments in the river');
xlabel('Distance from WWTP(m)');
ylabel('I-131 concentration in sediments(Bq/kg[dry mass])');
hold all;
errorbar(xx,rr,errorrr,'rd');
hold all;
errorbar(0,28.3,1.72,'bd'); %plot of the 2012 data
legend ('Model simulation','Experimental data 2008-
2009','Experimental data 2012');
```